PRETRAIN–TEST TASK ALIGNMENT GOVERNS GENERALIZATION IN IN-CONTEXT LEARNING

Anonymous authors
Paper under double-blind review

ABSTRACT

In-context learning (ICL) is a central capability of Transformer models, but the structures in data that enable its emergence and govern its robustness remain poorly understood. In this work, we study how the structure of pretraining tasks governs generalization in ICL. Using a solvable model for ICL of linear regression by linear attention, we derive an exact expression for ICL generalization error in high dimensions under arbitrary pretraining–testing task covariance mismatch. This leads to a new alignment measure that quantifies how much information about the pretraining task distribution is useful for inference at test time. We show that this measure directly predicts ICL performance not only in the solvable model but also in nonlinear Transformers. Our analysis further reveals a tradeoff between specialization and generalization in ICL: depending on task distribution alignment, increasing pretraining task diversity can either improve or harm test performance. Together, these results identify train-test task alignment as a key determinant of generalization in ICL.

1 INTRODUCTION

Pre-training on simple next-token prediction enables Transformer models to acquire a remarkably broad array of capabilities, from language translation to code generation and mathematical reasoning (Achiam et al., 2023; Anthropic, 2024; DeepSeek-AI et al., 2025; Vaswani et al., 2017). Among the emergent abilities that enable Transformers to flexibly execute a myriad of tasks, their capacity for in-context learning (ICL) is particularly striking, as it allows for test-time task execution without task-specific pretraining (Von Oswald et al., 2023; Wei et al., 2022). In other words, ICL reflects the ability to emergently meta-learn a learning algorithm during pretraining, which is then applied to learn from data within a context at test time (Akyürek et al., 2023; Raventós et al., 2023; Zhang et al., 2024a).

For ICL to be effective, the tasks encountered at test time must not be totally unrelated to those encountered during pretraining, as there is no free lunch. Though substantial theoretical attention has been devoted to the question of why and how ICL emerges and how well the resulting algorithms perform, this key issue of how pretraining tasks should be selected to enable ICL in the real, test-time world remains underexplored (Lu et al., 2025; Zhang et al., 2024a;b). This motivates the central question of our work:

Central Question

How does mismatch between the structure of tasks seen in pretraining and the structure of tasks faced at test time affect the ability of in-context learners to generalize?

Here, we investigate how pretrain-test task alignment affects generalization in a simple model setting, ICL of linear regression. Our main contributions are as follows:

- We give a precise mathematical analysis of the performance of a simplified linear Attention module learning to do linear regression in-context. We model pretraining and test task distributions with arbitrary covariance structure, generalizing previous works on this model that assumed identical task distributions (Lu et al., 2025; Zhang et al., 2024a). In this solvable model, ICL generalization is governed by a particular alignment metric between pretraining and test task distributions.

- Though derived for a simplified linear model, we show that this alignment measure predicts the generalization performance of nonlinear Transformers trained to do linear regression in-context.
- Finally we show in the solvable model that it is not always optimal from a generalization standpoint to pretrain on the same distribution of tasks that the model will encounter at test time, as echoed in kernel regression (Canatar et al., 2022).

In all, our work sheds light on how pretrain-test task alignment shapes the performance of in-context algorithms. It reveals how the inductive biases of Transformers can result in optimal task *misalignment*: rather than teaching to the test, a different curriculum of pretraining tasks may better enable a Transformer to learn the algorithm that enables it to generalize well at test time.

1.1 Related Work

Empirical studies of ICL. Empirical work has shown that LLMs can learn diverse tasks from examples alone, with performance improving predictably with scale (Achiam et al., 2023; Anthropic, 2024; DeepSeek-AI et al., 2025; Vaswani et al., 2017; Von Oswald et al., 2023; Wei et al., 2022). Several studies document how architectural components, such as attention heads or MLP layers, are recruited during training to implement ICL (Kratsios & Furuya, 2025; Reddy, 2024; Tong & Pehlevan, 2025; Zhang et al., 2024b). Various works have also focused on understanding what algorithms transformers can learn to perform, including gradient descent, Bayesian inference, and compression. (Ahn et al., 2023; Cole et al., 2025; Elmoznino et al., 2025; Lee et al., 2025; Liu et al., 2024; Mahankali et al., 2023; McCracken et al., 2025; Shen et al., 2025; Singh et al., 2023; Wurgaft et al., 2025; Zhang et al., 2023). Others have explored the role of task diversity in shaping generalization, showing that diverse pretraining induces transitions from memorization to generalization (Raventós et al., 2023). The specific effect of data structure and its role in ICL emergence has also been studied empirically, notably by Chan et al. (2022) highlighting the importance of *anisotropic* data for the emergence of ICL abilities. Our work provides a theoretical counterpart to these empirical investigations, as we model the generalization effects of structured task distributions.

Theoretical studies of ICL. Theoretical work has flourished in simplified Transformer models, particularly with linear or kernelized attention. A number of studies show that these architectures can implement classical learning algorithms, including kernel regression, ridge regression, or gradient descent, purely from in-context tokens (Akyürek et al., 2023; Bai et al., 2023; Li et al., 2023; Von Oswald et al., 2023; Zhang et al., 2024b). These insights have advanced our mechanistic understanding of ICL as algorithm emulation. However, most of these works make restrictive assumptions. Commonly, data is drawn from isotropic Gaussians, train and test distributions are matched, and generalization is studied only in the infinite-sample or population limit. Even recent studies of finite-sample ICL retain these simplifying assumptions *i.e.* without full generality of training and testing task distribution (Fu et al., 2023; Li et al., 2024; Lu et al., 2025; Zhang et al., 2024b). A notable exception is the work of Goddard et al. (2025) that studies tasks sampled from separate portions of a spherical task manifold. Our work advances this "task generalization" frontier by deriving an exact expression for the ICL generalization error in the presence of arbitrary task covariances and finite-sample regimes. This allows us to explore how task-structure mismatch affects generalization, a setting largely absent from prior theoretical models.

Train-Test task alignment in other settings. Outside of ICL, the idea of train-test task alignment in linear regression has been studied in the context of out-of-distribution generalization under target vector and covariate shifts. In particular, past works have studied which measures of alignment between train and test feature covariance matrices determine out-of-distribution generalization in high-dimensional ridge regression (Atanasov et al., 2025; Canatar et al., 2021b; Patil et al., 2024; Tripuraneni et al., 2021). These works build on a substantial body of results showing how the generalization performance of ridge regression is determined by the structure of the training feature covariance—principal directions with larger population variance are learned first—and the alignment of the task vector with those high-variance directions (Advani et al., 2020; Atanasov et al., 2024; Canatar et al., 2021a; Dobriban & Wager, 2015; Hastie et al., 2022). Our work brings this perspective into the ICL setting by analyzing the effects of the pretraining covariance, and pretrain-test misalignment on generalization. We show that even in simple linear regression settings, struc-

ture mismatch induces rich, nontrivial behavior, reinforcing the broader principle that distributional alignment between pretraining and test-time data is a key driver of generalization.

2 Model Setup

We begin by setting up the solvable model used to derive the results of this work. This setup builds on previous works that apply a reduced-parameter version of linear attention to linear regression ICL (Lu et al., 2025; Wang et al., 2020; Wu et al., 2024; Zhang et al., 2024a).

ICL of linear regression. We consider an in-context regression task: the input to the model is a sequence of the form $\{\boldsymbol{x}_1, y_1, \boldsymbol{x}_2, y_2, \ldots, \boldsymbol{x}_\ell, y_\ell, \boldsymbol{x}_{\ell+1}\}$, and the required output is the matching $y_{\ell+1}$ corresponding to $\boldsymbol{x}_{\ell+1}$. This input is called a context, and ℓ the context length. We consider the case that the relationship between $\boldsymbol{x}$ and y is approximately linear:

$$y_i = \langle \boldsymbol{x}_i, \boldsymbol{w} \rangle + \epsilon_i \tag{1}$$

for noise ϵ_i and task vector $\boldsymbol{w}$. Thus, the model needs to form an estimate of $\boldsymbol{w}$ using $\{\boldsymbol{x}_1, y_1, \boldsymbol{x}_2, y_2, \ldots, \boldsymbol{x}_\ell, y_\ell\}$ and then apply it to $\boldsymbol{x}_{\ell+1}$ to estimate $y_{\ell+1}$.

Pretraining data. The pretraining data batch will contain n sample sequences of the above form, *i.e.*, for $\mu = 1, ..., n$, the μth sample sequence $\{\boldsymbol{x}_1, y_1, \boldsymbol{x}_2, y_2, \ldots, \boldsymbol{x}_\ell, y_\ell, \boldsymbol{x}_{\ell+1}\}$ related by the approximate linear mapping from (1), $y_i^\mu = \langle \boldsymbol{x}_i^\mu, \boldsymbol{w}^\mu \rangle + \epsilon_i^\mu$, where now $\boldsymbol{w}^\mu$ is the task vector corresponding to the μ-th sample context.

We will sample the pretraining batch as follows: For $i = 1, \ldots, \ell$ and $\mu = 1, \ldots, n$,

$$\begin{aligned} \boldsymbol{x}_i^\mu &\sim_{\text{i.i.d.}} \mathcal{N}(0, I_d/d)\,, \qquad & \epsilon_i^\mu &\sim_{\text{i.i.d.}} \mathcal{N}(0, \rho)\,, \\ \boldsymbol{w}^\mu &\sim_{\text{unif}} \{\boldsymbol{t}_1\,, \cdots, \boldsymbol{t}_k\} \qquad & \text{where } \boldsymbol{t}_j &\sim_{\text{i.i.d.}} \mathcal{N}(0, C_{\text{train}}) \text{ for } j = 1, \ldots, k\,. \end{aligned} \tag{2}$$

The parameter k here is called *task diversity*. Note that if $k < n$, the pretraining batch contains some tasks repeated across the contexts. In this way, we control both the amount k of actually unique tasks seen during pretraining, as well as the structure of the task distribution using C_{train}. This distinguishes our setup from previous studies which typically focus on isotropic or matched tasks (Fu et al., 2023; Li et al., 2024; Lu et al., 2025; Raventós et al., 2023).

Linear attention. We will study the performance of the linear self-attention block (Wang et al., 2020) on this in-context regression task. The input to the linear self-attention model is an embedding matrix Z made up of our context sequence. Here, following the convention of Wang et al. (2020); Wu et al. (2024); Zhang et al. (2024a), we chose to embed $\{\boldsymbol{x}_1, y_1, \boldsymbol{x}_2, y_2, \ldots, \boldsymbol{x}_\ell, y_\ell, \boldsymbol{x}_{\ell+1}\}$ as

$$Z = \begin{bmatrix} \boldsymbol{x}_1 & \boldsymbol{x}_2 & \ldots & \boldsymbol{x}_\ell & \boldsymbol{x}_{\ell+1} \\ y_1 & y_2 & \ldots & y_\ell & 0 \end{bmatrix} \in \mathbb{R}^{(d+1)\times(\ell+1)}, \tag{3}$$

where 0 in the lower-right corner is a placeholder token for the $y_{\ell+1}$ we wish to predict. The model's output (Katharopoulos et al., 2020; Shen et al., 2021; Wang et al., 2020) is given by

$$A = Z + VZ(KZ)^\top (QZ)/\ell \tag{4}$$

for value matrix $V \in \mathbb{R}^{(d+1)\times(d+1)}$ and key, query matrices K, Q such that $K^\top Q \in \mathbb{R}^{(d+1)\times(d+1)}$. Following the positional encoding in (3), the linear attention model's prediction for $y_{\ell+1}$ is

$$\hat{y} = A_{d+1,\ell+1}. \tag{5}$$

Previous works from Zhang et al. (2024a) and Lu et al. (2025) have shown that the output $\hat{y} = A_{d+1,\ell+1}$ of the model can be reduced to give a simpler, analytically-tractable model. Writing the attention and value matrices as

$$V = \begin{bmatrix} V_{11} & \boldsymbol{v}_{12} \\ \boldsymbol{v}_{21}^\top & v_{22} \end{bmatrix}, \quad M = \begin{bmatrix} M_{11} & \boldsymbol{m}_{12} \\ \boldsymbol{m}_{21}^\top & m_{22} \end{bmatrix} \equiv K^\top Q\,, \tag{6}$$

the predictor expands as

$$\hat{y} = \frac{1}{\ell} \boldsymbol{x}_{\ell+1}^\top \left(v_{22} M_{11}^\top \sum_{i=1}^{\ell} y_i \boldsymbol{x}_i + v_{22} \boldsymbol{m}_{21} \sum_{i=1}^{\ell} y_i^2 + M_{11}^\top \sum_{i=1}^{\ell+1} \boldsymbol{x}_i \boldsymbol{x}_i^\top \boldsymbol{v}_{21} + \boldsymbol{m}_{21} \sum_{i=1}^{\ell} y_i \boldsymbol{x}_i^\top \boldsymbol{v}_{21} \right). \tag{7}$$

Zhang et al. (2024a) and Lu et al. (2025) argued that that the final two terms depending on $\boldsymbol{v}_{21}$ can be removed without affecting the performance of the estimator: the first, depending on $\boldsymbol{x}_i \boldsymbol{x}_i^\top \boldsymbol{v}_{21}$, does not contain any task information, and thus does not help us estimate $\boldsymbol{w}$. The second, depending

on $y_i \boldsymbol{x}_i^\top \boldsymbol{v}_{21}$ provides only a one-dimensional projection of $\boldsymbol{x}$ and $\boldsymbol{w}$, and so for large-dimensional tokens, does not effectively contribute to good estimate of $\boldsymbol{w}$ either. For this reason, we set $\boldsymbol{v}_{21} = \boldsymbol{0}$. Zhang et al. (2024a) showed that this choice of parameter initialization is stable under SGD, further validating this assumption. With this simplification, we can rewrite the simplified model's output as

$$\hat{y}_{\ell+1} = \mathrm{tr}(\Gamma H_Z^\top) \tag{8}$$

for a parameter matrix

$$\Gamma \equiv v_{22} \begin{bmatrix} M_{11}^\top / d & \boldsymbol{m}_{21} \end{bmatrix} \in \mathbb{R}^{d \times (d+1)} . \tag{9}$$

and a data matrix

$$H_Z \equiv \boldsymbol{x}_{\ell+1} \begin{bmatrix} \frac{d}{\ell} \sum_{i \le \ell} y_i \boldsymbol{x}_i^\top & \frac{1}{\ell} \sum_{i \le \ell} y_i^2 \end{bmatrix} \in \mathbb{R}^{d \times (d+1)}. \tag{10}$$

Reduced model optimization. Given a batch $\{\boldsymbol{x}_1^\mu, y_1^\mu, \ldots, \boldsymbol{x}_{\ell+1}^\mu, y_{\ell+1}^\mu\}_{\mu=1}^n$ of pretraining data (as explained above), we can find finite-sample optimal parameters by minimizing MSE loss on next-output prediction with ridge regularization, giving

$$\Gamma^* = \arg\min_\Gamma \sum_{\mu=1}^n \left(y_{\ell+1}^\mu - \mathrm{tr}(\Gamma (H^\mu)^\top) \right)^2 + \frac{n}{d} \lambda \, \mathrm{tr}(\Gamma \Gamma^\top) , \tag{11}$$

where $\lambda > 0$ is a regularization parameter, and H^μ is defined by (10) for the μth context. We will focus on the minimum-norm predictor, *i.e.*, on the limit where $\lambda \to 0$ (Hastie et al., 2022).

Test error. We finally wish to test the pretrained model on a general task to see if the model can genuinely perform in-context regression. The test distribution $\mathcal{P}_{\text{test}}$ is then

$$\boldsymbol{x}_i^{\text{test}} \sim_{\text{i.i.d.}} \mathcal{N}(0, I_d/d) , \qquad \epsilon_i^{\text{test}} \sim_{\text{i.i.d.}} \mathcal{N}(0, \rho) , \qquad \boldsymbol{w}^{\text{test}} \sim_{\text{i.i.d.}} \mathcal{N}(0, C_{\text{test}}) . \tag{12}$$

We will measure ICL performance by the average MSE error of our optimal estimator $\hat{y}_{\ell+1}^* = \mathrm{tr}(\Gamma^* H^\top)$ over the test distribution,

$$\mathcal{E}_{\text{ICL}}(\Gamma^*) = \mathbb{E}_{\mathcal{P}_{\text{test}}}[(y_{\ell+1} - \mathrm{tr}(\Gamma^* H^\top))^2] . \tag{13}$$

We highlight here the generality of the test task distribution through the new matrix C_{test}, allowing us to study the interaction of training and testing task structure.

Data parameters in the high-dimensional limit. We have introduced four data parameters: token dimension d, context length ℓ, pretraining batch size n, and task diversity k. As is standard in the theory of high-dimensional regression (Advani et al., 2020; Atanasov et al., 2024; Hastie et al., 2022; Lu et al., 2025), we will consider a scaling limit where all four of these parameters are taken to infinity in a way such that the following ratios remain constant:

$$\frac{\ell}{d} \equiv \alpha, \qquad \frac{n}{d^2} \equiv \tau, \qquad \text{and} \quad \frac{k}{d} \equiv \kappa. \tag{14}$$

Considering this limit makes the model analytically tractable, but preserves interesting phenomena that are present at finite size. Going forward, we will refer to α, τ, and κ as the context length, batch size, and task diversity parameters, respectively.

Pretraining task quantities. Before presenting our formula for this ICL test error, it will be helpful to first define some task-distribution quantities, which depend on the pretraining task covariance C_{train} and task diversity parameter κ. These quantities effectively tell us how well we can reconstruct C_{train} from the k-sample task covariance that the model sees during pretraining,

$$R_k = \frac{1}{k} \sum_{j \in [k]} \boldsymbol{t}_j \boldsymbol{t}_j^\top .$$

Because the pretraining tasks $\{\boldsymbol{t}_1, ..., \boldsymbol{t}_k\}$ are random, R_k is a random matrix. However, in high dimensions, the following *deterministic* quantities capture the relevant information about R_k: let the deterministic matrix $F_\kappa(z)$ and deterministic scalar $\mathcal{M}_\kappa(z)$ be defined through the implicit equations

$$F_\kappa(z) = \left(\left(1 - \frac{1}{\kappa} + \frac{z}{\kappa} \mathcal{M}_\kappa(z) \right) C_{\text{train}} + z I_d \right)^{-1} \tag{15}$$

$$\mathcal{M}_\kappa(z) = \mathrm{tr}[F_\kappa(z)] . \tag{16}$$

Then, we have the high-dimensional equivalence

$$(R_k + z I_d)^{-1} \simeq F_\kappa(z). \tag{17}$$

As we define formally in Definition 1 of Appendix B, this equivalence holds in the sense that the traces of $(R_k + zI_d)^{-1}$ and $F_\kappa(z)$ against test matrices coincide in the high-dimensional limit. Here, $z \in \mathbb{R}_+$ is a noise threshold parameter suppressing smaller eigenvalues of R_k.

Intuitively, $F_\kappa(z)$ and $\mathcal{M}_\kappa(z)$ give us information about how much signal in C_{train} can be recovered after a finite number k of pretraining samples, filtered by noise level z. As $z \to 0$ and $\kappa \to \infty$, R_k approaches C_{train}, and we therefore fully recover the original distribution of tasks. We will use $F'_\kappa(z)$ to refer to the derivative of $F_\kappa(z)$ with respect to z; this gives a measure of the sensitivity of this covariance recovery matrix to the noise level z. These quantities will play a key role in our discussion of task alignment.

Given this setup, we compute a formula for the ICL generalization error $\mathcal{E}_{\text{ICL}}(\Gamma^*)$ in terms of the data parameters α, κ, τ, the pretraining task covariance C_{train}, and the testing task covariance C_{test}. We present this formula and discuss its implications in the following sections.

Notation. We write $\text{tr}[A] \equiv \text{tr}(A)/d$ for the dimension-scaled trace of matrix A. We use a normalized Frobenius inner product between two matrices, *i.e.* $\langle A, B \rangle \equiv \text{tr}[AB^\top] = \text{tr}(AB^\top)/d$. We abbreviate the normalized traces of the task covariances as $c_{\text{train}} = \text{tr}[C_{\text{train}}]$ and $c_{\text{test}} = \text{tr}[C_{\text{test}}]$. We denote high-dimensional equivalence (as in Appendix Definition 1) by $\simeq$.

3 ICL Test Error Depends on Task Misalignment

3.1 Task alignment determines generalization in the solvable model

We state the main result of our analysis of the simplified linear attention model, which is an analytical formula for the ICL error (13) in high dimensions. Here we give only an informal statement of this result and focus on its implications; the formal statement is given by (C.2) in Appendix C.

Result: High-dimensional formula for the ICL error $\mathcal{E}(\Gamma^*)$

The ICL test error (13) of the simplified linear attention model set up above is given by

$$\mathcal{E}_{\text{ICL}}(\Gamma^*) \simeq e_{\text{scalar}}(\boldsymbol{\lambda}_{\text{train}}, c_{\text{test}}) + e_{\text{misalign}}(C_{\text{train}}, C_{\text{test}}) \equiv e_{\text{ICL}}(C_{\text{train}}, C_{\text{test}}) \tag{18}$$

in the high-dimensional limit, where

$$e_{\text{misalign}}(C_{\text{train}}, C_{\text{test}}) = \langle C_{\text{test}},\ \mathcal{K} \rangle \tag{19}$$

measures the alignment between C_{test} and

$$\mathcal{K} \equiv qF_\kappa(\sigma) + (q\tilde{\lambda} - \sigma^2)F'_\kappa(\sigma). \tag{20}$$

Appearing in this formula are an effective ridge variable $\tilde{\lambda}$ and effective noise variable σ given by the solution of the joint equations

$$\tilde{\lambda}\mathcal{M}_\kappa(\sigma) = 1 - \tau \quad \text{for } \tau < 1\,, \qquad \tilde{\lambda} = 0 \quad \text{for } \tau > 1 \tag{21}$$

$$\sigma = (\rho + c_{\text{train}})/\alpha + \tilde{\lambda}\,. \tag{22}$$

where $\mathcal{M}_\kappa(\cdot)$ is determined self-consistently as in (16). Finally q is a pretraining-error term given by (C.10) and $e_{\text{scalar}}(\boldsymbol{\lambda}_{\text{train}}, c_{\text{test}})$ is given by (C.12); note that both q and e_{scalar} only depend on C_{test} through its trace c_{test}, and e_{scalar} only depends on C_{train} through its spectrum $\boldsymbol{\lambda}_{\text{train}}$.

We first support this result through Figure 1, which shows agreement between our theory curve formula $e_{\text{ICL}}(C_{\text{train}}, C_{\text{test}})$ and numerical simulations of MSE error $\mathcal{E}_{\text{ICL}}(\Gamma^*)$ given by (11) and the test distribution (12). By comparing the left (e_{ICL}) and right (e_{misalign}) panels of Figure 1 we see that the behavior of e_{ICL} is highly dependent on the e_{misalign} term: for well-aligned training and testing distributions, low and decreasing e_{misalign} in κ immediately leads to a monotonic decrease in e_{ICL} in κ; for worse-aligned training and testing distributions, e_{ICL} can be nonmonotonic or even monotonically increasing in κ. This is intriguing, as one would naïvely expect additional task samples to improve in-context performance, but this is not true in general: whether additional task samples are helpful for ICL depends on the alignment of the pretraining and testing distributions.

To gain intuition for this misalignment error (19), a useful analogy is to consider the simplest matrix "misalignment" measure $\langle C_{\text{test}} C_{\text{train}}^{-1} \rangle$. Firstly, this measure captures misalignment that can occur

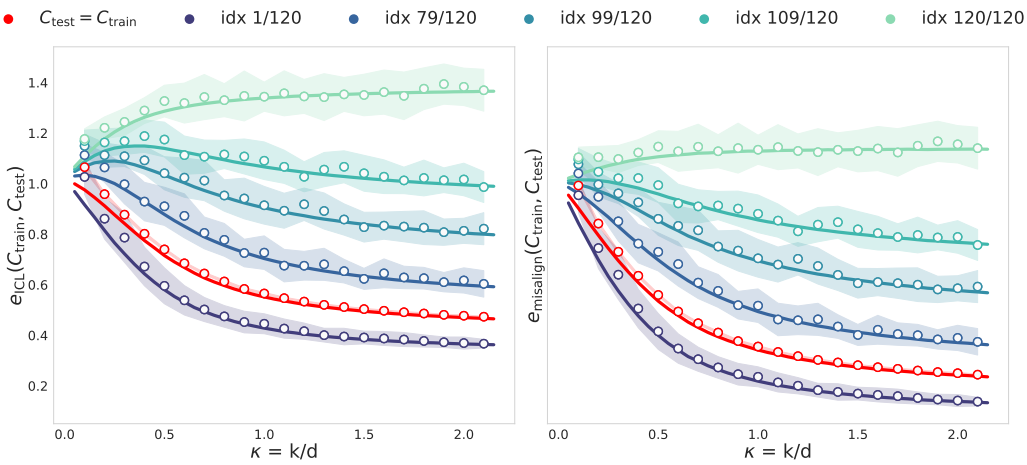

Figure 1: Theoretical e_{ICL} (left panel) and e_{misalign} (right panel) curves plotted against numerical simulations of $\mathcal{E}(\Gamma^*)$ computed directly from sampled data. We choose C_{train} with uniform eigenvalue distribution: $C_{\text{train}} \propto \text{diag}([d, d-1, \cdots, 1])$ such that $\text{tr}(C_{\text{train}}) = d$. We compare $C_{\text{test}} = C_{\text{train}}$ (red curves) with testing on single task directions, *i.e.*, the "`idx i/d`" labels correspond to rank-1 test covariances $C_{\text{test}}^i = d\boldsymbol{e}_i\boldsymbol{e}_i^\top$ spiked at index i. In this way, C_{test}^1 captures the strongest task direction of C_{train} and C_{test}^d captures the weakest. *Parameters:* $d = 120$, $\alpha = 2$, $\tau = 4$, $\rho = 0.01$. Shading represents $\pm$std of numerical simulations. We calculate the simulation values of e_{misalign} in the right panel by subtracting e_{scalar} from the MSE simulation values $\mathcal{E}(\Gamma^*)$.

from misalignment of the *eigenvectors* of C_{test} and C_{train}; see Corollary 4.1 and its proof for further discussion. Going beyond eigenvectors, because the eigenvalues of C_{train}^{-1} are ordered opposite to the eigenvalues of C_{train}, this measure effectively captures the relative strength of signal directions between C_{test} and C_{train}: if C_{train} and C_{test} share the same eigenvalues, alignment will be maximized when these eigenvalues appear in the same order, and minimized when these eigenvalues appear in opposing orders. This is precisely why $\langle C_{\text{test}}C_{\text{train}}^{-1}\rangle$ can be interpreted as a misalignment measure, as even this very simple *Ansatz* shows how misalignment arises from mismatches in the relative weighting of signal directions between train and test tasks. This relative strength argument holds for our alignment measure, where instead of $\langle C_{\text{test}}C_{\text{train}}^{-1}\rangle$ we use $\langle C_{\text{test}}\mathcal{K}\rangle$. Here $\mathcal{K}$ obviously depends on C_{train}—they share the same eigenvectors—and importantly, has the same property as C_{train}^{-1} that its eigenvalues are oppositely ordered to the eigenvalues of C_{train} (see Appendix D).

However, this eigenvalue-ordering argument is incomplete for the ICL setting. It assumes that C_{train} can be fully learned, but with finite context length, finite task diversity, and label noise, this cannot be the case. Thus, the model cannot access the full covariance structure, only a partial version, whose resolution depends on both sampling and noise. This is precisely what the resolvent terms $F_\kappa(\cdot)$ and $F'_\kappa(\cdot)$ in $\mathcal{K}$ can capture, as explained in the setup. This is analogous to the alignment measures that emerge in ordinary ridge regression under covariate shift, which capture how much of the training feature covariance can be resolved from finitely many samples (Atanasov et al., 2025; Canatar et al., 2021b; Patil et al., 2024; Tripuraneni et al., 2021). Furthermore, the effective noise σ must play a key role in alignment, as the model does not know *a priori* that this is an "in-context" learning problem, and must learn to decouple the tokens from the task for each context in order to extract the task information implicit in that context. The ability of the model to do this depends on both the label noise (ρ), the context length (α), and a sufficient number of contexts ($\tilde{\lambda}$). In fact, the form of $\sigma = (\rho + \text{tr}[C_{\text{train}}])/\alpha + \tilde{\lambda}$ is also familiar from ordinary ridge regression as an effective noise-to-signal term: the optimal ridge regularization parameter balances the variance due to label noise (ρ) with the estimation error from having finite data (Atanasov et al., 2024; Canatar et al., 2021a; Hastie et al., 2022; Patil et al., 2024). At infinite sample size, the optimal ridge is simply ρ, the label noise. However, at finite sample size, the effective regularization is increased due to the finite-sample estimation error, and becomes $(\rho + \sigma_w^2)/\alpha$, where σ_w^2 characterizes variability or complexity of the regression task. In the same way, our model has to resolve the statistics of the tokens $\boldsymbol{x}$ over samples (ℓ, measured by α), and so we expect terms familiar from linear regression to appear in our formula.

In summary, our alignment measure is motivated both by arguments regarding spectral ordering and relative strength, as well as having all components necessary to capture finite size effects. In Figure 2 we compare our alignment measure to three others: the population matrix measure $\langle C_{\text{train}} C_{\text{test}}^{-1} \rangle$, a simpler version of our alignment measure involving just the resolvent $\langle C_{\text{train}} F_\kappa(\sigma) \rangle$, and finally the Centered Kernel Alignment (CKA) measure (Kornblith et al., 2019). This comparison illustrates how different measures emphasize different aspects: $\langle C_{\text{train}} F_\kappa(\sigma) \rangle$ accounts for finite-sample resolution effects but not as specifically as $\langle C_{\text{train}} \mathcal{K} \rangle$ does, while $\langle C_{\text{train}} C_{\text{test}}^{-1} \rangle$ and CKA both miss finite-sample effects altogether, CKA instead being designed to detect nonlinear representational similarity. We perform this comparison by first noting that, trivially, e_{misalign} is monotonically related to e_{ICL}: larger e_{misalign} implies larger e_{ICL}. Figure 2 shows e_{ICL} for fixed C_{train} and varying C_{test} plotted against the above matrix alignment measures between C_{train} and C_{test}. We see that $\langle C_{\text{train}} \mathcal{K} \rangle$ and $\langle C_{\text{train}} F_\kappa(\sigma) \rangle$ are the strongest drivers of e_{ICL} (*i.e.* most monotonically related, with $\langle C_{\text{train}} \mathcal{K} \rangle$ obviously being perfectly correlated), while the performance of $\langle C_{\text{test}} C_{\text{train}}^{-1} \rangle$ and CKA as predictors of e_{ICL} is lacking.

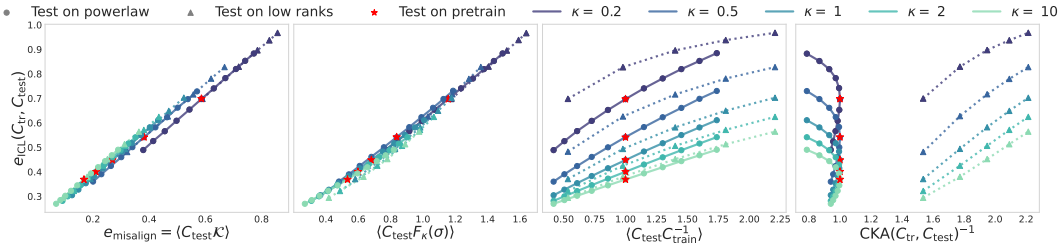

Figure 2: $e_{\text{ICL}}(C_{\text{train}}, C_{\text{test}})$ against alignment measures: $e_{\text{misalign}}(C_{\text{train}}, C_{\text{test}})$, $\text{tr}[C_{\text{test}} F]$, $\text{tr}[C_{\text{test}} C_{\text{train}}^{-1}]$, and $1/\text{CKA}(C_{\text{train}}, C_{\text{test}})$ from left to right. C_{train} is fixed to be a diagonal matrix with powerlaw spectrum $C_{\text{train}} \propto \text{diag}([1^{-p}, ..., d^{-p}]$ with power $p = 0.9$ and $\text{tr}[C_{\text{train}}] = 1$. C_{test} is varied over a range of different covariance matrices that are simultaneously diagonalizable with C_{train}, specifically power spectrum with different powers (circles connected by solid line), and low-rank covariance matrices $C_r = \text{diag}[(d/r)\mathbf{1}_r, \mathbf{0}_{d-r}]$ (triangular markers connected by dashed line). Changing the power of the powerlaw tests or the rank of the low-rank tests will make them either more or less aligned with C_{train}. *Parameters:* $d = 120$, $\alpha = 2$, $\tau = 4$, $\rho = 0.01$.

3.2 Task alignment predicts generalization in nonlinear Transformers

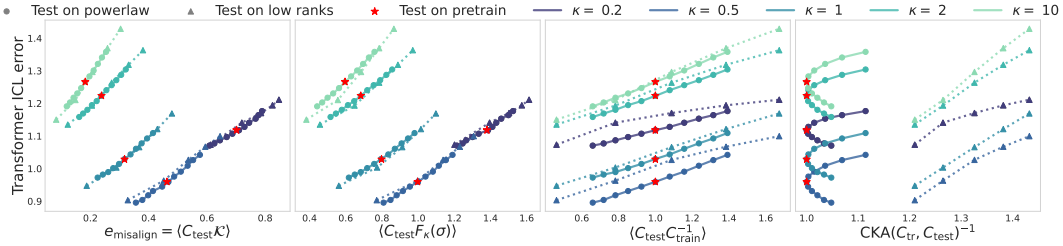

Figure 3: ICL test loss of a nonlinear transformer against different alignment measures. The setup of the covariances is identical to Figure 2, the only difference is that here ICL error is computed as the MSE on the test task as performed by a trained two-layer architecture with softmax attention and MLP connections. Our measure e_{misalign} achieves the best correlation with ICL error: the Spearman coefficients (measuring monotonicity, over all test covariances and averaged over the different κ values) are **0.99 (ours)**, 0.98, 0.96, and 0.39 from left to right. *Parameters:* $d = 20$, $\alpha = 2$, $\tau = 4$, $\rho = 0.01$.

We further support the predictive power of our alignment measure defined by e_{misalign} for ICL error in a two-layer transformer architecture with softmax attention by Figure 3. See Appendix H for details on the architecture setup. We see that even for an architecture far from the linear attention considered by the theory, our theoretically-derived alignment measure is still the best predictor of how changing the test distribution affects ICL error, compared to other alignment measures.

4 Mismatched Task Distributions Are Often Optimal

We have identified the relevant measure of alignment between the pretraining and testing task distributions for linear transformers learning to perform ICL. It is then natural to ask whether for a fixed test distribution C_{test}, is it always optimal to pretrain on the test distribution, *i.e.*, is $e_{\text{ICL}}(C_{\text{test}}, C_{\text{test}}) \leq e_{\text{ICL}}(C_{\text{train}}, C_{\text{test}})$? In this section, we show that the answer to this question is in general no, it is *not* always optimal to pretrain on the test distribution.

Covariance Alignment and Eigenspace Structure. We first show that it suffices to consider the case in which C_{train} and C_{test} are co-diagonalizable, as the ICL error is extremal in this case. Note that we can focus on e_{misalign}, as other terms in the ICL error (18) contained in e_{scalar} (C.12) are independent of the eigenvectors of these two matrices.

Corollary 4.1: Eigenspace alignment extremizes misalignment error

The misalignment error $e_{\text{misalign}}(C_{\text{train}}, C_{\text{test}}) = \langle C_{\text{test}}, \mathcal{K} \rangle$ is extremized when C_{test} and C_{train} are co-diagonalizable. Concretely, letting $\lambda_1(C_{\text{test}}) \geq \cdots \geq \lambda_d(C_{\text{test}})$ and $\lambda_1(\mathcal{K}) \geq \cdots \geq \lambda_d(\mathcal{K})$ be the ordered eigenvalues of these two real symmetric matrices, we have

$$\frac{1}{d}\sum_{j=1}^{d} \lambda_j(C_{\text{test}})\lambda_{d-j+1}(\mathcal{K}) \leq e_{\text{misalign}} \leq \frac{1}{d}\sum_{j=1}^{d} \lambda_j(C_{\text{test}})\lambda_j(\mathcal{K}), \tag{23}$$

with equality in either the upper or lower bound if and only if C_{train} and C_{test} are co-diagonalizable.

To show that this result holds, we observe that, as C_{test} and $\mathcal{K}$ are real symmetric matrices, the desired bound (23) is simply a restatement of Ruhe's trace inequality normalized by $1/d$, where equality holds if and only if C_{test} and $\mathcal{K}$ are co-diagonalizable. We give a self-contained proof of this inequality in Appendix E (see also Marshall et al. (2010) or Li (2020)'s expository blog post). By its definition (20), $\mathcal{K}$ and C_{train} have the same eigenvectors, so the claim follows.

Therefore, the misalignment error can be minimized *or* maximized if we assume that C_{train} and C_{test} are simultaneously diagonalizable. We therefore restrict our attention to the co-diagonalizable setting, and write the ordered eigenvalues of C_{train} and C_{test} as $\lambda_1(C_{\text{train}}) \geq \cdots \geq \lambda_d(C_{\text{train}})$ and $\lambda_1(C_{\text{test}}) \geq \cdots \geq \lambda_d(C_{\text{test}})$, respectively.

Optimal Test Covariance for Fixed Pretraining Distribution. Before presenting results on optimal pretraining structure for fixed task structure, which is a more practical question to answer, we begin first with a simpler question: For fixed training distribution C_{train}, is it always optimal to test on the pretraining distribution, *i.e.*, is $e_{\text{ICL}}(C_{\text{train}}, C_{\text{train}}) \leq e_{\text{ICL}}(C_{\text{train}}, C_{\text{test}})$? The following result answers this question in the negative:

Corollary 4.2: Trace-constrained optimal test covariance

For fixed C_{train} and fixed $c_{\text{train}} = c_{\text{test}}$, we have that $e_{\text{ICL}}(C_{\text{train}}, C_{\text{test}})$ is minimized by the single-index spike covariance with eigenvalues

$$[\lambda_1(C_{\text{test}}) \quad \cdots \quad \lambda_i(C_{\text{test}}) \quad \cdots \quad \lambda_d(C_{\text{test}})] = [dc_{\text{train}} \quad \cdots \quad 0 \quad \cdots \quad 0]$$

i.e., all test signal is aligned with the largest eigenvector of C_{train}.

To see that this holds, note that $e_{\text{ICL}}(C_{\text{train}}, C_{\text{test}})$ is a linear function of the eigenvalues of C_{test} as $e_{\text{misalign}}(C_{\text{train}}, C_{\text{test}})$ is linear in C_{test} and $e_{\text{scalar}}(\boldsymbol{\lambda}_{\text{train}}, c_{\text{test}})$ does not depend on C_{test} when $c_{\text{test}} = c_{\text{train}}$. Furthermore, the constraint $c_{\text{test}} = c_{\text{train}}$ is a simplex in the space of C_{test} eigenvalues. The minimum will thus be attained along the simplex, at the vertex corresponding to the lowest eigenvalue of $\mathcal{K}$. As argued in Appendix D, this corresponds to the largest eigenvalue of C_{train}.

This result illustrates a bias towards exploiting low-dimensional structure seen in pretraining to optimize performance at test time. In these cases, where we are optimizing test structure C_{test} for a fixed pretraining structure C_{train}, we observe that the best generalization is achieved by concentrating all signal into a single shared direction, collapsing the task manifold into a single dimension. In other

words, it is easier to learn to generalize over a degenerate low-rank test structure highly aligned to the pretraining structure than to generalize over the entire pretraining structure learned from limited samples. This is familiar from spectral bias results of ordinary ridge regression (Canatar et al., 2021a;b). Note that, had our training distribution been isotropic ($C_{\text{train}} = I_d$) then all trace-fixed test covariances will perform equally; utilizing anisotropy is crucial.

Non-Optimality of Pretraining on Test Structure We now investigate the original question of the optimal pretraining task covariance C_{train}, given a particular test task covariance C_{test}. We will provide an example showing it is in fact *not optimal* in general to have $C_{\text{train}} = C_{\text{test}}$. We particularly emphasize that whether or not a particular task structure is better for pretraining depends strongly on the task diversity κ.

Consider the case of power-law task distributions at both training and test time, *i.e.*,

$$C_{\text{train}} \propto \text{diag}\left[1^{-p_{\text{train}}} \quad \cdots \quad d^{-p_{\text{train}}}\right], \qquad C_{\text{test}} \propto \text{diag}\left[1^{-p_{\text{test}}} \quad \cdots \quad d^{-p_{\text{test}}}\right], \tag{24}$$

with the normalization constant chosen such that $\text{tr}[C_{\text{train}}] = \text{tr}[C_{\text{test}}]$. We can study the effect of changing C_{train} relative to C_{test} on e_{ICL} by changing the exponent p_{train} relative to fixed p_{test}.

Figure 4 shows that, for low κ, pretraining on C_{train} with higher spectral power relative to the test power can improve ICL error. We see that focusing pretraining on a low-dimensional subspace, effectively creating a strong inductive bias, can improve in-context learning performance when training data is scarce. The model generalizes better by overfitting to fewer directions, rather than learning more directions weakly. However, increasing the pretraining power too much relative to the test power will worsen ICL performance, as the pretraining task set is now too low-dimensional to cover enough variation at test time. We highlight that the potential advantage coming from increasing training spectral power weakens as soon as κ is large enough for the model to be able to resolve enough task directions during pretraining.

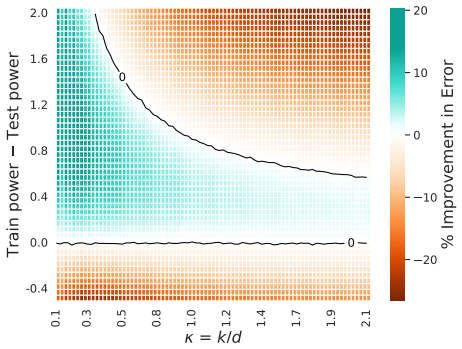

Figure 4: Heatmap of theoretical ICL error given by (18) for simultaneously diagonalizable powerlaw task covariances C_{train} and C_{test} with spectral power p_{train} (variable) and p_{test} (fixed). The x-axis shows task diversity κ and the y-axis shows the difference $p_{\text{train}} - p_{\text{test}}$ between task spectral powers. The colourbar shows the % improvement in error by training on C_{train} instead of C_{test}. This shows that increasing spectral power in the pretraining tasks can markedly improve ICL error on the same test distribution. *Parameters:* $d = 100$, $p_{\text{test}} = 0.9$, $\alpha = 1$, $\tau = 4$, $\rho = 0.01$.

5 Conclusions

We have developed a framework of in-context task alignment, showing that our derived measure of *error from task misalignment* is a robust predictor of ICL performance, even in nonlinear architectures. This derivation builds on a model of in-context learning of linear regression, which we extend to *fully general* task covariates. Previous works have shown that the performance of ICL models can suffer under task shift, particularly in cases of low task diversity (Garg et al., 2022; Goddard et al., 2025; Zhang et al., 2024a). We highlight that, while task misalignment is provably a driver of ICL error, our fully-general covariance framework can be used to show that task misalignment can indeed be utilized to *improve* ICL performance in cases of limited data.

Looking forward, our analysis provides a rich model of ICL with many further avenues of investigation. A more detailed analysis of the interaction between pretraining-specific error e_{scalar} and misalignment error e_{misalign} could be used to derive a general heuristic for optimal pretraining, with potential implications for practical settings. Beyond task alignment, additional highly relevant phenomena can be investigated: we highlight (1) a generalized learning transition in task diversity (empirically studied by Raventós et al. (2023); see Appendix F) and (2) test-time scaling (see Gozeten et al. (2025) and Appendix G). We leave exploration of these phenomena to future work.

REFERENCES

Josh Achiam, Steven Adler, Sandhini Agarwal, Lama Ahmad, Ilge Akkaya, Florencia Leoni Aleman, Diogo Almeida, Janko Altenschmidt, Sam Altman, Shyamal Anadkat, et al. Gpt-4 technical report. *arXiv preprint arXiv:2303.08774*, 2023.

Madhu S Advani, Andrew M Saxe, and Haim Sompolinsky. High-dimensional dynamics of generalization error in neural networks. *Neural Networks*, 132:428–446, 2020. doi: https://doi.org/10.1016/j.neunet.2020.08.022. URL https://www.sciencedirect.com/science/article/pii/S0893608020303117.

Kwangjun Ahn, Xiang Cheng, Hadi Daneshmand, and Suvrit Sra. Transformers learn to implement preconditioned gradient descent for in-context learning, 2023. URL https://arxiv.org/abs/2306.00297.

Ekin Akyürek, Dale Schuurmans, Jacob Andreas, Tengyu Ma, and Denny Zhou. What learning algorithm is in-context learning? investigations with linear models. In *The Eleventh International Conference on Learning Representations*, 2023. URL https://openreview.net/forum?id=0g0X4H8yN4I.

Anthropic. The claude 3 model family: Opus, sonnet, haiku, 2024. URL https://api.semanticscholar.org/CorpusID:268232499.

Alexander Atanasov, Jacob A Zavatone-Veth, and Cengiz Pehlevan. Risk and cross validation in ridge regression with correlated samples. In *Forty-second International Conference on Machine Learning*, 2025. URL https://openreview.net/forum?id=GMwKpJ9TiR.

Alexander B. Atanasov, Jacob A. Zavatone-Veth, and Cengiz Pehlevan. Scaling and renormalization in high-dimensional regression. *arXiv*, 2024.

Yu Bai, Fan Chen, Huan Wang, Caiming Xiong, and Song Mei. Transformers as statisticians: Provable in-context learning with in-context algorithm selection. In A. Oh, T. Naumann, A. Globerson, K. Saenko, M. Hardt, and S. Levine (eds.), *Advances in Neural Information Processing Systems*, volume 36, pp. 57125–57211. Curran Associates, Inc., 2023. URL https://proceedings.neurips.cc/paper_files/paper/2023/file/b2e63e36c57e153b9015fece2352a9f9-Paper-Conference.pdf.

Abdulkadir Canatar, Blake Bordelon, and Cengiz Pehlevan. Spectral bias and task-model alignment explain generalization in kernel regression and infinitely wide neural networks. *Nature Communications*, 12(1), May 2021a. ISSN 2041-1723. doi: 10.1038/s41467-021-23103-1. URL http://dx.doi.org/10.1038/s41467-021-23103-1.

Abdulkadir Canatar, Blake Bordelon, and Cengiz Pehlevan. Out-of-distribution generalization in kernel regression. In M. Ranzato, A. Beygelzimer, Y. Dauphin, P.S. Liang, and J. Wortman Vaughan (eds.), *Advances in Neural Information Processing Systems*, volume 34, pp. 12600–12612. Curran Associates, Inc., 2021b. URL https://proceedings.neurips.cc/paper_files/paper/2021/file/691dcb1d65f31967a874d18383b9da75-Paper.pdf.

Abdulkadir Canatar, Blake Bordelon, and Cengiz Pehlevan. Out-of-distribution generalization in kernel regression, 2022. URL https://arxiv.org/abs/2106.02261.

Stephanie C. Y. Chan, Adam Santoro, Andrew K. Lampinen, Jane X. Wang, Aaditya Singh, Pierre H. Richemond, Jay McClelland, and Felix Hill. Data distributional properties drive emergent in-context learning in transformers, 2022.

Frank Cole, Yulong Lu, Tianhao Zhang, and Yuxuan Zhao. In-context learning of linear dynamical systems with transformers: Error bounds and depth-separation, 2025. URL https://arxiv.org/abs/2502.08136.

DeepSeek-AI, Daya Guo, Dejian Yang, Haowei Zhang, Junxiao Song, Ruoyu Zhang, Runxin Xu, Qihao Zhu, Shirong Ma, Peiyi Wang, Xiao Bi, Xiaokang Zhang, Xingkai Yu, Yu Wu, Z. F. Wu, Zhibin Gou, Zhihong Shao, Zhuoshu Li, Ziyi Gao, Aixin Liu, Bing Xue, Bingxuan Wang, Bochao

Wu, Bei Feng, Chengda Lu, Chenggang Zhao, Chengqi Deng, Chenyu Zhang, Chong Ruan, Damai Dai, Deli Chen, Dongjie Ji, Erhang Li, Fangyun Lin, Fucong Dai, Fuli Luo, Guangbo Hao, Guanting Chen, Guowei Li, H. Zhang, Han Bao, Hanwei Xu, Haocheng Wang, Honghui Ding, Huajian Xin, Huazuo Gao, Hui Qu, Hui Li, Jianzhong Guo, Jiashi Li, Jiawei Wang, Jingchang Chen, Jingyang Yuan, Junjie Qiu, Junlong Li, J. L. Cai, Jiaqi Ni, Jian Liang, Jin Chen, Kai Dong, Kai Hu, Kaige Gao, Kang Guan, Kexin Huang, Kuai Yu, Lean Wang, Lecong Zhang, Liang Zhao, Litong Wang, Liyue Zhang, Lei Xu, Leyi Xia, Mingchuan Zhang, Minghua Zhang, Minghui Tang, Meng Li, Miaojun Wang, Mingming Li, Ning Tian, Panpan Huang, Peng Zhang, Qiancheng Wang, Qinyu Chen, Qiushi Du, Ruiqi Ge, Ruisong Zhang, Ruizhe Pan, Runji Wang, R. J. Chen, R. L. Jin, Ruyi Chen, Shanghao Lu, Shangyan Zhou, Shanhuang Chen, Shengfeng Ye, Shiyu Wang, Shuiping Yu, Shunfeng Zhou, Shuting Pan, S. S. Li, Shuang Zhou, Shaoqing Wu, Shengfeng Ye, Tao Yun, Tian Pei, Tianyu Sun, T. Wang, Wangding Zeng, Wanjia Zhao, Wen Liu, Wenfeng Liang, Wenjun Gao, Wenqin Yu, Wentao Zhang, W. L. Xiao, Wei An, Xiaodong Liu, Xiaohan Wang, Xiaokang Chen, Xiaotao Nie, Xin Cheng, Xin Liu, Xin Xie, Xingchao Liu, Xinyu Yang, Xinyuan Li, Xuecheng Su, Xuheng Lin, X. Q. Li, Xiangyue Jin, Xiaojin Shen, Xiaosha Chen, Xiaowen Sun, Xiaoxiang Wang, Xinnan Song, Xinyi Zhou, Xianzu Wang, Xinxia Shan, Y. K. Li, Y. Q. Wang, Y. X. Wei, Yang Zhang, Yanhong Xu, Yao Li, Yao Zhao, Yaofeng Sun, Yaohui Wang, Yi Yu, Yichao Zhang, Yifan Shi, Yiliang Xiong, Ying He, Yishi Piao, Yisong Wang, Yixuan Tan, Yiyang Ma, Yiyuan Liu, Yongqiang Guo, Yuan Ou, Yuduan Wang, Yue Gong, Yuheng Zou, Yujia He, Yunfan Xiong, Yuxiang Luo, Yuxiang You, Yuxuan Liu, Yuyang Zhou, Y. X. Zhu, Yanhong Xu, Yanping Huang, Yaohui Li, Yi Zheng, Yuchen Zhu, Yunxian Ma, Ying Tang, Yukun Zha, Yuting Yan, Z. Z. Ren, Zehui Ren, Zhangli Sha, Zhe Fu, Zhean Xu, Zhenda Xie, Zhengyan Zhang, Zhewen Hao, Zhicheng Ma, Zhigang Yan, Zhiyu Wu, Zihui Gu, Zijia Zhu, Zijun Liu, Zilin Li, Ziwei Xie, Ziyang Song, Zizheng Pan, Zhen Huang, Zhipeng Xu, Zhongyu Zhang, and Zhen Zhang. Deepseek-r1: Incentivizing reasoning capability in llms via reinforcement learning. *arXiv*, 2025. URL https://arxiv.org/abs/2501.12948.

Edgar Dobriban and Stefan Wager. High-dimensional asymptotics of prediction: Ridge regression and classification, 2015. URL https://arxiv.org/abs/1507.03003.

Eric Elmoznino, Tom Marty, Tejas Kasetty, Leo Gagnon, Sarthak Mittal, Mahan Fathi, Dhanya Sridhar, and Guillaume Lajoie. In-context learning and occam's razor, 2025. URL https://arxiv.org/abs/2410.14086.

Deqing Fu, Tian-Qi Chen, Robin Jia, and Vatsal Sharan. Transformers learn higher-order optimization methods for in-context learning: A study with linear models, 2023.

Shivam Garg, Dimitris Tsipras, Percy Liang, and Gregory Valiant. What can transformers learn in-context? a case study of simple function classes. In Alice H. Oh, Alekh Agarwal, Danielle Belgrave, and Kyunghyun Cho (eds.), *Advances in Neural Information Processing Systems*, 2022. URL https://openreview.net/forum?id=flNZJ2eOet.

Chase Goddard, Lindsay M. Smith, Vudtiwat Ngampruetikorn, and David J. Schwab. When can in-context learning generalize out of task distribution?, 2025. URL https://arxiv.org/abs/2506.05574.

Halil Alperen Gozeten, M. Emrullah Ildiz, Xuechen Zhang, Mahdi Soltanolkotabi, Marco Mondelli, and Samet Oymak. Test-time training provably improves transformers as in-context learners, 2025. URL https://arxiv.org/abs/2503.11842.

Trevor Hastie, Andrea Montanari, Saharon Rosset, and Ryan J. Tibshirani. Surprises in high-dimensional ridgeless least squares interpolation. *The Annals of Statistics*, 50(2):949 – 986, 2022. doi: 10.1214/21-AOS2133. URL https://doi.org/10.1214/21-AOS2133.

Angelos Katharopoulos, Apoorv Vyas, Nikolaos Pappas, and François Fleuret. Transformers are RNNs: Fast autoregressive transformers with linear attention. In *International conference on machine learning*, pp. 5156–5165. PMLR, 2020.

Simon Kornblith, Mohammad Norouzi, Honglak Lee, and Geoffrey Hinton. Similarity of neural network representations revisited, 2019. URL https://arxiv.org/abs/1905.00414.

Anastasis Kratsios and Takashi Furuya. Is in-context universality enough? mlps are also universal in-context, 2025. URL https://arxiv.org/abs/2502.03327.

Jin Hwa Lee, Andrew Kyle Lampinen, Aaditya K Singh, and Andrew M Saxe. Distinct computations emerge from compositional curricula in in-context learning. In *Workshop on Spurious Correlation and Shortcut Learning: Foundations and Solutions*, 2025. URL https://openreview.net/forum?id=oo5TNikeJl.

Yingcong Li, M. Emrullah Ildiz, Dimitris Papailiopoulos, and Samet Oymak. Transformers as algorithms: Generalization and stability in in-context learning, 2023.

Yingcong Li, Ankit Singh Rawat, and Samet Oymak. Fine-grained analysis of in-context linear estimation: Data, architecture, and beyond. In A. Globerson, L. Mackey, D. Belgrave, A. Fan, U. Paquet, J. Tomczak, and C. Zhang (eds.), *Advances in Neural Information Processing Systems*, volume 37, pp. 138324–138364. Curran Associates, Inc., 2024. URL https://proceedings.neurips.cc/paper_files/paper/2024/file/f9dc462382fef56d58279e75de2438f3-Paper-Conference.pdf.

Yingzhou Li. Von Neumann's trace inequalities. online blog post, 2020. URL: https://yingzhouli.com/posts/2020-07/von-neumann-trace-inequalities.html.

Toni J.b. Liu, Nicolas Boulle, Raphaël Sarfati, and Christopher Earls. Llms learn governing principles of dynamical systems, revealing an in-context neural scaling law. In *Proceedings of the 2024 Conference on Empirical Methods in Natural Language Processing*, pp. 15097–15117. Association for Computational Linguistics, 2024. doi: 10.18653/v1/2024.emnlp-main.842. URL http://dx.doi.org/10.18653/v1/2024.emnlp-main.842.

Yue M. Lu, Mary Letey, Jacob A. Zavatone-Veth, Anindita Maiti, and Cengiz Pehlevan. Asymptotic theory of in-context learning by linear attention. *Proceedings of the National Academy of Sciences*, 122(28):e2502599122, 2025. doi: 10.1073/pnas.2502599122. URL https://www.pnas.org/doi/abs/10.1073/pnas.2502599122.

Arvind Mahankali, Tatsunori B. Hashimoto, and Tengyu Ma. One step of gradient descent is provably the optimal in-context learner with one layer of linear self-attention, 2023. URL https://arxiv.org/abs/2307.03576.

Albert W. Marshall, Ingram Olkin, and Barry C. Arnold. *Inequalities: Theory of Majorization and Its Applications*. Springer New York, NY, 2 edition, 2010. doi: https://doi.org/10.1007/978-0-387-68276-1.

Gavin McCracken, Gabriela Moisescu-Pareja, Vincent Letourneau, Doina Precup, and Jonathan Love. Uncovering a universal abstract algorithm for modular addition in neural networks, 2025. URL https://arxiv.org/abs/2505.18266.

Pratik Patil, Jin-Hong Du, and Ryan Tibshirani. Optimal ridge regularization for out-of-distribution prediction. In Ruslan Salakhutdinov, Zico Kolter, Katherine Heller, Adrian Weller, Nuria Oliver, Jonathan Scarlett, and Felix Berkenkamp (eds.), *Proceedings of the 41st International Conference on Machine Learning*, volume 235 of *Proceedings of Machine Learning Research*, pp. 39908–39954. PMLR, 21–27 Jul 2024. URL https://proceedings.mlr.press/v235/patil24a.html.

Allan Raventós, Mansheej Paul, Feng Chen, and Surya Ganguli. Pretraining task diversity and the emergence of non-bayesian in-context learning for regression. In A. Oh, T. Naumann, A. Globerson, K. Saenko, M. Hardt, and S. Levine (eds.), *Advances in Neural Information Processing Systems*, volume 36, pp. 14228–14246. Curran Associates, Inc., 2023. URL https://proceedings.neurips.cc/paper_files/paper/2023/file/2e10b2c2e1aa4f8083c37dfe269873f8-Paper-Conference.pdf.

Gautam Reddy. The mechanistic basis of data dependence and abrupt learning in an in-context classification task. In *The Twelfth International Conference on Learning Representations*, 2024. URL https://openreview.net/forum?id=aN4Jf6Cx69.

Zhaiming Shen, Alexander Hsu, Rongjie Lai, and Wenjing Liao. Understanding in-context learning on structured manifolds: Bridging attention to kernel methods, 2025. URL https://arxiv.org/abs/2506.10959.

Zhuoran Shen, Mingyuan Zhang, Haiyu Zhao, Shuai Yi, and Hongsheng Li. Efficient attention: Attention with linear complexities. In *Proceedings of the IEEE/CVF winter conference on applications of computer vision*, pp. 3531–3539, 2021.

Aaditya K. Singh, Stephanie C. Y. Chan, Ted Moskovitz, Erin Grant, Andrew M. Saxe, and Felix Hill. The transient nature of emergent in-context learning in transformers, 2023. URL https://arxiv.org/abs/2311.08360.

William L. Tong and Cengiz Pehlevan. MLPs learn in-context on regression and classification tasks. In *The Thirteenth International Conference on Learning Representations*, 2025. URL https://openreview.net/forum?id=MbX0t1rUlp.

Nilesh Tripuraneni, Ben Adlam, and Jeffrey Pennington. Covariate shift in high-dimensional random feature regression. *arXiv*, 2021. URL https://arxiv.org/abs/2111.08234.

Ashish Vaswani, Noam Shazeer, Niki Parmar, Jakob Uszkoreit, Llion Jones, Aidan N Gomez, Łukasz Kaiser, and Illia Polosukhin. Attention is all you need. *Advances in neural information processing systems*, 30, 2017.

Johannes Von Oswald, Eyvind Niklasson, Ettore Randazzo, João Sacramento, Alexander Mordvintsev, Andrey Zhmoginov, and Max Vladymyrov. Transformers learn in-context by gradient descent. In Andreas Krause, Emma Brunskill, Kyunghyun Cho, Barbara Engelhardt, Sivan Sabato, and Jonathan Scarlett (eds.), *Proceedings of the 40th International Conference on Machine Learning*, volume 202 of *Proceedings of Machine Learning Research*, pp. 35151–35174. PMLR, 23–29 Jul 2023. URL https://proceedings.mlr.press/v202/von-oswald23a.html.

Sinong Wang, Belinda Z. Li, Madian Khabsa, Han Fang, and Hao Ma. Linformer: Self-attention with linear complexity, 2020.

Jason Wei, Yi Tay, Rishi Bommasani, Colin Raffel, Barret Zoph, Sebastian Borgeaud, Dani Yogatama, Maarten Bosma, Denny Zhou, Donald Metzler, Ed H. Chi, Tatsunori Hashimoto, Oriol Vinyals, Percy Liang, Jeff Dean, and William Fedus. Emergent abilities of large language models. *Transactions on Machine Learning Research*, 2022. ISSN 2835-8856. URL https://openreview.net/forum?id=yzkSU5zdwD.

Jingfeng Wu, Difan Zou, Zixiang Chen, Vladimir Braverman, Quanquan Gu, and Peter Bartlett. How many pretraining tasks are needed for in-context learning of linear regression? In *The Twelfth International Conference on Learning Representations*, 2024. URL https://openreview.net/forum?id=vSh5ePa0ph.

Daniel Wurgaft, Ekdeep Singh Lubana, Core Francisco Park, Hidenori Tanaka, Gautam Reddy, and Noah D. Goodman. In-context learning strategies emerge rationally, 2025. URL https://arxiv.org/abs/2506.17859.

Ruiqi Zhang, Spencer Frei, and Peter L. Bartlett. Trained transformers learn linear models in-context. *Journal of Machine Learning Research*, 25(49):1–55, 2024a. URL http://jmlr.org/papers/v25/23-1042.html.

Ruiqi Zhang, Jingfeng Wu, and Peter L. Bartlett. In-context learning of a linear transformer block: Benefits of the mlp component and one-step gd initialization, 2024b.

Yufeng Zhang, Fengzhuo Zhang, Zhuoran Yang, and Zhaoran Wang. What and how does in-context learning learn? bayesian model averaging, parameterization, and generalization, 2023. URL https://arxiv.org/abs/2305.19420.

SUPPLEMENTARY INFORMATION

In the following sections, we provide proofs of the results presented in the main document. We begin in Section A with some preliminary simplifications of the ICL and IDG population risk for general Γ. Then in Section B we will set up and complete the random matrix theory calculation necessary to justify our main result, equation 18, which will be done in Section C. Section E will cover the proof of the phenomena-based Corollary 4.1. Then, we provide additional analysis of transitions in the behavior of the ICL error as a function of the task diversity κ in Section F, and of shifts in the test-time context length in Section G. We conclude with details of our numerical experiments in Section H.

Notation Here $\mathrm{vec}(\cdot)$ will mean the vectorization operation under the *row-major* convention: for a $d_1 \times d_2$ matrix A, $\mathrm{vec}(A)$ is a vector in $\mathbb{R}^{d_1 d_2}$, formed by stacking the rows of A together. We will use this together with the matrix Kronecker product $\otimes$, where by standard results we have

$$\mathrm{vec}(uv^\top) = u \otimes v \tag{25}$$

$$(u \otimes v)(w \otimes s)^\top = (uw^\top) \otimes (vs^\top)\,. \tag{26}$$

We will also use the notation $[M]_{\setminus 0}$ to mean the principal minor of a matrix M (*i.e.*, first row and column removed). We use the following normalized trace

$$\mathrm{tr}[A] \equiv \frac{1}{d}\,\mathrm{tr}(A)\,.$$

We use $\equiv$ when defining new quantities. We use $\simeq$ for *deterministic equivalence*, which describes the large-dimensional limit of a random quantity (either a scalar or matrix) that concentrates to a deterministic value as dimension approaches infinity.

A GENERAL ERROR FORMULAS

Here we will set up the definition of various test errors more generally than in the main document. As this is an in-context learning setup, there are different types of "generalization" that can be studied: generalization over the tokens and generalization over the tasks. We will define two test errors to capture these separately.

In general, we wish to understand the performance and behavior of this estimator Γ^*, which is pretrained on data from the pretraining distribution $\mathcal{P}_{\mathrm{train}}$, when tested on new data. Namely, we will analyze the average performance of an estimator $\hat{y} = \mathrm{tr}(\Gamma, H_Z)$ as a function of given fixed Γ under the MSE loss, which is the natural loss for a regression test. The most general this expression can be is

$$\mathcal{L}_{\mathrm{MSE}}(\Gamma) = \mathbb{E}_{\mathcal{P}_{\mathrm{test}}}\left[(y_{\ell+1} - \mathrm{tr}(\Gamma, H_Z))^2\right] \tag{A.1}$$

for a general test distribution $\mathcal{P}_{\mathrm{test}}$ detailing how to sample tokens x, tasks w, and noise ϵ at test time.

We will consider two different testing regimes: the *in-context learning (ICL)* test, where the model sees new tasks w, and the *in-distribution generalization (IDG)* (or *in-weights*) test, where the model sees the *exact same tasks* used in pretraining $\{\boldsymbol{t}_1, \cdots, \boldsymbol{t}_k\}$, where each $\boldsymbol{t}_j \sim_{\text{i.i.d.}} \mathcal{N}(0, C_{\mathrm{train}})$. Explicitly, we define these test distributions and corresponding error functions as follows:

$$\mathcal{E}_{\mathrm{IDG}}(\Gamma) = \mathbb{E}_{\mathcal{P}_{\mathrm{IDG}}}\left[(y_{\ell+1} - \mathrm{tr}(\Gamma, H_Z))^2\right] \tag{A.2}$$

$$\mathcal{P}_{\mathrm{IDG}} := \boldsymbol{x}_i^\mu \sim_{\text{i.i.d.}} \mathcal{N}(0, I_d/d)\,, \quad \boldsymbol{w}^\mu \sim_{\text{unif}} \{\boldsymbol{t}_1, \cdots, \boldsymbol{t}_k\}\,, \quad \epsilon_i^\mu \sim_{\text{i.i.d.}} \mathcal{N}(0, \rho)\,,$$

where $i \in [\ell]$ and $\mu \in [n]$, and

$$\mathcal{E}_{\mathrm{ICL}}(\Gamma) = \mathbb{E}_{\mathcal{P}_{\mathrm{ICL}}}\left[(y_{\ell+1} - \mathrm{tr}(\Gamma, H_Z))^2\right] \tag{A.3}$$

$$\mathcal{P}_{\mathrm{ICL}} := \boldsymbol{x}_i^\mu \sim_{\text{i.i.d.}} \mathcal{N}(0, I_d/d)\,, \quad \boldsymbol{w}^\mu \sim_{\text{i.i.d.}} \mathcal{N}(0, C_{\mathrm{test}})\,, \quad \epsilon_i^\mu \sim_{\text{i.i.d.}} \mathcal{N}(0, \rho)\,,$$

where $i \in [\ell_{\mathrm{test}}]$ and $\mu \in [n]$.

Notice here that we've introduced two different context lengths: ℓ for the IDG distribution, which is the same context length as the pretraining setup $\mathcal{P}_{\mathrm{train}}$ given by (2), and ℓ_{test} which is the context length at testing time. This allows us to later explore the effect of pretraining and testing on sequences of different context lengths.

We assume that both task covariance matrices C_{train} and C_{test} are well-behaved in high dimensions, specifically that $\text{tr}[C_{\text{train}}], \text{tr}[C_{\text{test}}] = \Theta(1)$. This ensures the task signals are not over or under amplified as $d \to \infty$.

Lemma 1. ***Simplified test losses.*** *Consider IDG and ICL test distribution and corresponding error functions as given by (A.2) and (A.3). For fixed parameters $\Gamma \in \mathbb{R}^{d\times(d+1)}$ and data sampled according to test distribution $\mathcal{P}_{\text{IDG}}$ or $\mathcal{P}_{\text{ICL}}$, the corresponding errors e_{IDG} and e_{ICL} can be expressed as*

$$\mathcal{E}_{\text{IDG}}(\Gamma) \simeq \rho + \text{tr}[\Sigma R_k] - 2\,\text{tr}[\Gamma A_{\text{IDG}}^\top] + \text{tr}[\Sigma\Gamma B_{\text{IDG}}\Gamma^\top] \tag{A.4}$$

$$\mathcal{E}_{\text{ICL}}(\Gamma) \simeq \rho + \text{tr}[\Sigma C_{\text{test}}] - 2\,\text{tr}[\Gamma A_{\text{ICL}}^\top] + \text{tr}[\Sigma\Gamma B_{\text{ICL}}\Gamma^\top] \tag{A.5}$$

where

$$A_{\text{IDG}} = \begin{bmatrix}\Sigma R_k\Sigma & (\text{tr}[\Sigma R_k] + \rho)\,\Sigma \boldsymbol{b}_k\end{bmatrix}, \tag{A.6}$$

$$A_{\text{ICL}} = \begin{bmatrix}\Sigma C_{\text{test}}\Sigma & 0\end{bmatrix}, \tag{A.7}$$

$$B_{\text{IDG}} = \begin{bmatrix}\Sigma R_k\Sigma + \frac{d}{\ell}\left(\text{tr}[\Sigma R_k] + \rho\right)\Sigma & (\text{tr}[\Sigma R_k] + \rho)\,\Sigma\boldsymbol{b}_k \\ (\text{tr}[\Sigma R_k] + \rho)\,(\Sigma\boldsymbol{b}_k)^\top & (\text{tr}[\Sigma R_k] + \rho)^2\end{bmatrix} \tag{A.8}$$

$$B_{\text{ICL}} = \begin{bmatrix}\Sigma C_{\text{test}}\Sigma + \frac{d}{\ell_{\text{test}}}\left(\text{tr}[\Sigma C_{\text{test}}] + \rho\right)\Sigma & 0 \\ 0^\top & (\text{tr}[\Sigma C_{\text{test}}] + \rho)^2\end{bmatrix} \tag{A.9}$$

for $\boldsymbol{b}_k$ and R_k defined by the pretraining task sample $\{w_1, \ldots, w_k\}$ as

$$\boldsymbol{b}_k = \frac{1}{k}\sum_{j\in[k]} \boldsymbol{t}_j\,, \qquad R_k = \frac{1}{k}\sum_{j\in[k]} \boldsymbol{t}_j\boldsymbol{t}_j^\top\,. \tag{A.10}$$

The "$\simeq$" in these formulas comes from ignoring terms of order $1/d$ and weaker, i.e. a high-dimensional treatment.

Remark 1. *Note that Result 1 is a more general result than the setting considered in the main paper, as Result 1 allows for general token covariance Σ. The rest of this work will take $\Sigma = I_d$ for computational tractability.*

Lemma 2. *Fix the task vector w that defines $y_i = \boldsymbol{w}^\top\boldsymbol{x}_i + \epsilon_i$ for context Z. Denote the conditional expectation over only $\boldsymbol{x}_i, \epsilon_i$, holding $\boldsymbol{w}$ fixed, by $\mathbb{E}_{\boldsymbol{x},\epsilon}$. Then we have the following*

$$\mathbb{E}_{\boldsymbol{x},\epsilon}[y_{\ell+1}] = 0 \tag{A.11}$$

$$\mathbb{E}_{\boldsymbol{x},\epsilon}[H_Z] = 0 \tag{A.12}$$

$$\mathbb{E}_{\boldsymbol{x},\epsilon}[y_{\ell+1}^2] = \text{tr}[\Sigma\boldsymbol{w}\boldsymbol{w}^\top] + \rho \tag{A.13}$$

$$\mathbb{E}_{\boldsymbol{x},\epsilon}[y_{\ell+1}H_Z] = \frac{1}{d}\begin{bmatrix}\Sigma\boldsymbol{w}\boldsymbol{w}^\top\Sigma & \left(\text{tr}[\Sigma\boldsymbol{w}\boldsymbol{w}^\top] + \rho\right)\Sigma\boldsymbol{w}\end{bmatrix} \tag{A.14}$$

$$\mathbb{E}_{\boldsymbol{x},\epsilon}[\text{vec}(H_Z)\,\text{vec}(H_Z)^\top] \simeq \frac{1}{d}\Sigma\otimes\begin{bmatrix}\Sigma\boldsymbol{w}\boldsymbol{w}^\top\Sigma + \frac{d}{\ell}\left(\text{tr}[\Sigma\boldsymbol{w}\boldsymbol{w}^\top] + \rho\right)\Sigma & \left(\text{tr}[\Sigma\boldsymbol{w}\boldsymbol{w}^\top] + \rho\right)\Sigma\boldsymbol{w} \\ \left(\text{tr}[\Sigma\boldsymbol{w}\boldsymbol{w}^\top] + \rho\right)(\Sigma\boldsymbol{w})^\top & \left(\text{tr}[\Sigma\boldsymbol{w}\boldsymbol{w}^\top] + \rho\right)^2\end{bmatrix} \tag{A.15}$$

where recall

$$H_Z \equiv \boldsymbol{x}_{\ell+1}\begin{bmatrix}\frac{d}{\ell}\sum_{i\le\ell} y_i\boldsymbol{x}_i^\top & \frac{1}{\ell}\sum_{i\le\ell} y_i^2\end{bmatrix} \in \mathbb{R}^{d\times(d+1)}\,. \tag{A.16}$$

Proof. Equation (A.11) follows immediately from the linearity of $y_{\ell+1}$ in ϵ and $\boldsymbol{x}_i$, which are both mean-0 random variables. Similarly for (A.12), as H_Z is linear in $\boldsymbol{x}_{\ell+1}$.

For the conditional expectation of $y_{\ell+1}^2$ in (A.13), simply expand

$$\mathbb{E}_{\boldsymbol{x},\epsilon}\left[y_{\ell+1}^2\right] = \mathbb{E}_{\boldsymbol{x},\epsilon}\left[(\boldsymbol{w}^\top\boldsymbol{x}_{\ell+1} + \epsilon_{\ell+1})(\boldsymbol{x}_{\ell+1}^\top\boldsymbol{w} + \epsilon_{\ell+1})\right] \tag{A.17}$$

$$= \mathbb{E}_{\boldsymbol{x},\epsilon}\left[\boldsymbol{w}^\top\boldsymbol{x}_{\ell+1}\boldsymbol{x}_{\ell+1}^\top\boldsymbol{w} + \epsilon_{\ell+1}^2\right] \tag{A.18}$$

$$= \frac{1}{d}\boldsymbol{w}^\top\Sigma\boldsymbol{w} + \rho \tag{A.19}$$

$$= \text{tr}[\Sigma\boldsymbol{w}\boldsymbol{w}^\top] + \rho\,. \tag{A.20}$$

For (A.14), have

$$\mathbb{E}_{\boldsymbol{x},\epsilon}\left[\frac{d}{\ell}\sum_{i\le\ell} y_{\ell+1}y_i\boldsymbol{x}_{\ell+1}\boldsymbol{x}_i^\top\right] = \frac{d}{\ell}\sum_{i\le\ell}\mathbb{E}_{\boldsymbol{x},\epsilon}\left[\boldsymbol{x}_{\ell+1}(\boldsymbol{x}_{\ell+1}^\top\boldsymbol{w}+\epsilon_{\ell+1})(\boldsymbol{w}^\top\boldsymbol{x}_i+\epsilon_i)\boldsymbol{x}_i^\top\right] \tag{A.21}$$

$$= \frac{d}{\ell}\sum_{i\le\ell}\mathbb{E}_{\boldsymbol{x},\epsilon}\left[\boldsymbol{x}_{\ell+1}\boldsymbol{x}_{\ell+1}^\top\boldsymbol{w}\boldsymbol{w}^\top\boldsymbol{x}_i\boldsymbol{x}_i^\top\right] \tag{A.22}$$

$$= \frac{d}{\ell}\sum_{i\le\ell}(\Sigma/d)\,\boldsymbol{w}\boldsymbol{w}^\top\,(\Sigma/d) \tag{A.23}$$

$$= \frac{1}{d}\Sigma\boldsymbol{w}\boldsymbol{w}^\top\Sigma \tag{A.24}$$

and

$$\mathbb{E}_{\boldsymbol{x},\epsilon}\left[\frac{1}{\ell}\sum_{i\le\ell} y_{\ell+1}\boldsymbol{x}_{\ell+1}y_i^2\right] = \frac{1}{\ell}\sum_{i\le\ell}\mathbb{E}_{\boldsymbol{x},\epsilon}\left[\boldsymbol{x}_{\ell+1}(\boldsymbol{x}_{\ell+1}^\top\boldsymbol{w}+\epsilon_{\ell+1})(\boldsymbol{w}^\top\boldsymbol{x}_i+\epsilon_i)(\boldsymbol{x}_i^\top\boldsymbol{w}+\epsilon_i)\right] \tag{A.25}$$

$$= \frac{1}{\ell}\sum_{i\le\ell}\mathbb{E}_{\boldsymbol{x},\epsilon}\left[\boldsymbol{x}_{\ell+1}\boldsymbol{x}_{\ell+1}^\top\boldsymbol{w}(\boldsymbol{w}^\top\boldsymbol{x}_i\boldsymbol{x}_i^\top\boldsymbol{w}+\epsilon_i\epsilon_i)\right] \tag{A.26}$$

$$= \frac{1}{\ell}\sum_{i\le\ell}(\Sigma/d)\boldsymbol{w}(\boldsymbol{w}^\top(\Sigma/d)\boldsymbol{w}+\rho) \tag{A.27}$$

$$= \frac{1}{d}(\mathrm{tr}[\Sigma\boldsymbol{w}\boldsymbol{w}^\top]+\rho)\Sigma\boldsymbol{w} \tag{A.28}$$

as required for (A.14).

Finally, for (A.15,) first it will be helpful to note, by Isserlis's theorem / Wick's theorem, that

$$\mathbb{E}_{\boldsymbol{x},\epsilon}\left[\boldsymbol{x}_1\boldsymbol{x}_1^\top\boldsymbol{w}\boldsymbol{w}^\top\boldsymbol{x}_1\boldsymbol{x}_1^\top\right] = \frac{2}{d^2}\Sigma\boldsymbol{w}\boldsymbol{w}^\top\Sigma + \frac{1}{d}\,\mathrm{tr}[\Sigma\boldsymbol{w}\boldsymbol{w}^\top]\Sigma\,. \tag{A.29}$$

It will also be useful to rewrite

$$\mathrm{vec}(H_Z)\,\mathrm{vec}(H_Z)^\top = (\boldsymbol{x}_{\ell+1}\boldsymbol{x}_{\ell+1}^\top)\otimes\left(\begin{bmatrix}\frac{d}{\ell}\sum_{i\le\ell}y_i\boldsymbol{x}_i\\ \frac{1}{\ell}\sum_{i\le\ell}y_i^2\end{bmatrix}\begin{bmatrix}\frac{d}{\ell}\sum_{i\le\ell}y_i\boldsymbol{x}_i^\top & \frac{1}{\ell}\sum_{i\le\ell}y_i^2\end{bmatrix}\right)$$

by converting between $\mathrm{vec}()$ and matrix Kronecker. The components of this Kronecker product are independent and can therefore be averaged separately. Clearly

$$\mathbb{E}_{\boldsymbol{x},\epsilon}[\boldsymbol{x}_{\ell+1}\boldsymbol{x}_{\ell+1}^\top] = \frac{\Sigma}{d}\,,$$

so we focus on the second matrix in the product. This matrix will have blocks that sum over two ℓ sums, leading to both $\Theta(1)$ and $\Theta(1/\ell)$ terms in the final expression. We will ignore terms of order $1/\ell$ as we eventually will only use this formula in a proportional limit of $\ell, d \to \infty$ such that $\ell/d = \Theta(1)$, and thus $1/\ell$ is negligible in this limit.

We proceed block-by-block. Firstly,

$$\mathbb{E}_{\boldsymbol{x},\epsilon}\left[\frac{d^2}{\ell^2}\sum_{i,j\le\ell} y_i\boldsymbol{x}_i y_j\boldsymbol{x}_j^\top\right] = \frac{d^2}{\ell^2}\sum_i \mathbb{E}_{\boldsymbol{x},\epsilon}\left[\boldsymbol{x}_i(\boldsymbol{x}_i^\top\boldsymbol{w}+\epsilon_i)(\boldsymbol{w}^\top\boldsymbol{x}_i+\epsilon_i)\boldsymbol{x}_i^\top\right]$$
$$+\frac{d^2}{\ell^2}\sum_{i\neq j}\mathbb{E}_{\boldsymbol{x},\epsilon}\left[\boldsymbol{x}_i(\boldsymbol{x}_i^\top\boldsymbol{w}+\epsilon_i)(\boldsymbol{w}^\top\boldsymbol{x}_j+\epsilon_j)\boldsymbol{x}_j^\top\right] \tag{A.30}$$
$$=\ell\frac{d^2}{\ell^2}\mathbb{E}_{\boldsymbol{x},\epsilon}[\boldsymbol{x}_1\boldsymbol{x}_1^\top\boldsymbol{w}\boldsymbol{w}^\top\boldsymbol{x}_1\boldsymbol{x}_1^\top+\epsilon_!\epsilon_1\boldsymbol{x}_1\boldsymbol{x}_1^\top]$$
$$+(\ell^2-\ell)\frac{d^2}{\ell^2}\mathbb{E}_{\boldsymbol{x},\epsilon}[\boldsymbol{x}_1\boldsymbol{x}_1^\top\boldsymbol{w}\boldsymbol{w}^\top\boldsymbol{x}_2\boldsymbol{x}_2^\top] \tag{A.31}$$
$$=\ell\frac{d^2}{\ell^2}\left(\frac{1}{d}\operatorname{tr}[\Sigma\boldsymbol{w}\boldsymbol{w}^\top]\Sigma+\frac{2}{d^2}\Sigma\boldsymbol{w}\boldsymbol{w}^\top\Sigma+\frac{1}{d}\rho\Sigma\right)$$
$$+(\ell^2-\ell)\frac{d^2}{\ell^2}\left(\frac{1}{d^2}\Sigma\boldsymbol{w}\boldsymbol{w}^\top\Sigma\right) \tag{A.32}$$
$$=\left(1+\frac{1}{\ell}\right)\Sigma\boldsymbol{w}\boldsymbol{w}^\top\Sigma+\frac{d}{\ell}\left(\operatorname{tr}[\Sigma\boldsymbol{w}\boldsymbol{w}^\top]+\rho\right)\Sigma \tag{A.33}$$
$$\simeq\Sigma\boldsymbol{w}\boldsymbol{w}^\top\Sigma+\frac{d}{\ell}\left(\operatorname{tr}[\Sigma\boldsymbol{w}\boldsymbol{w}^\top]+\rho\right)\Sigma\,. \tag{A.34}$$

Secondly,

$$\mathbb{E}_{\boldsymbol{x},\epsilon}\left[\frac{d}{\ell^2}\sum_{i,j\le\ell} y_i\boldsymbol{x}_i y_j^2\right] = \ell\frac{d}{\ell^2}\mathbb{E}_{\boldsymbol{x},\epsilon}\left[\boldsymbol{x}_1 y_1^3\right]+(\ell^2-\ell)\frac{d}{\ell^2}\mathbb{E}_{\boldsymbol{x},\epsilon}\left[\boldsymbol{x}_1 y_1\right]\mathbb{E}_{\boldsymbol{x},\epsilon}\left[y_2^2\right] \tag{A.35}$$
$$=\frac{1}{\ell d}\left(d\operatorname{tr}[\Sigma\boldsymbol{w}\boldsymbol{w}^\top]\Sigma+2\Sigma\boldsymbol{w}\boldsymbol{w}^\top\Sigma\right)\boldsymbol{w}+3\frac{1}{\ell}\rho\Sigma\boldsymbol{w}$$
$$+\left(1-\frac{1}{\ell}\right)\left(\operatorname{tr}[\Sigma\boldsymbol{w}\boldsymbol{w}^\top]+\rho\right)\Sigma\boldsymbol{w} \tag{A.36}$$
$$\simeq\left(\operatorname{tr}[\Sigma\boldsymbol{w}\boldsymbol{w}^\top]+\rho\right)\Sigma\boldsymbol{w}\,. \tag{A.37}$$

Finally,

$$\mathbb{E}_{\boldsymbol{x},\epsilon}\left[\frac{1}{\ell^2}\sum_{i,j\le\ell} y_i^2 y_j^2\right] = \frac{1}{\ell}\mathbb{E}_{\boldsymbol{x},\epsilon}[y_1^4]+\frac{\ell^2-\ell}{\ell^2}\mathbb{E}_{\boldsymbol{x},\epsilon}[y_1^2]\mathbb{E}_{\boldsymbol{x},\epsilon}[y_2^2] \tag{A.38}$$
$$=\frac{1}{\ell}\left(\mathbb{E}_{\boldsymbol{x},\epsilon}[\boldsymbol{w}^\top xx^\top\boldsymbol{w}\boldsymbol{w}^\top\boldsymbol{x}\boldsymbol{x}^\top\boldsymbol{w}]+6\rho\mathbb{E}_x[\boldsymbol{w}^\top\boldsymbol{x}\boldsymbol{x}^\top\boldsymbol{w}]+3\rho^2\right)$$
$$+\left(1-\frac{1}{\ell}\right)\left(\operatorname{tr}[\Sigma\boldsymbol{w}\boldsymbol{w}^\top]+\rho\right)^2 \tag{A.39}$$
$$\simeq\left(\operatorname{tr}[\Sigma\boldsymbol{w}\boldsymbol{w}^\top]+\rho\right)^2\,. \tag{A.40}$$

Combining these pieces gives (A.15). □

Proof. **[of Lemma 1]** We begin by noting that for both IDG and ICL test errors, we can expand

$$e(\Gamma)=\mathbb{E}_{\boldsymbol{x},\boldsymbol{w},\epsilon}\left[\left(y_{\ell+1}-\operatorname{tr}(\Gamma H_Z^\top)\right)^2\right]=\mathbb{E}_{\boldsymbol{w}}\left[\mathbb{E}_{\boldsymbol{x},\epsilon}\left[\left(y_{\ell+1}-\operatorname{tr}(\Gamma H_Z^\top)\right)^2\right]\right]$$
$$=\mathbb{E}_{\boldsymbol{w}}\left[\mathbb{E}_{\boldsymbol{x},\epsilon}\left[\left(y_{\ell+1}-\operatorname{vec}(\Gamma)^\top\operatorname{vec}(H_Z)\right)^2\right]\right]$$
$$=\mathbb{E}_{\boldsymbol{w}}\left[\mathbb{E}_{\boldsymbol{x},\epsilon}\left[y_{\ell+1}^2\right]\right]-2\operatorname{vec}(\Gamma)^\top\mathbb{E}_{\boldsymbol{w}}\left[\mathbb{E}_{\boldsymbol{x},\epsilon}\left[y_{\ell+1}\operatorname{vec}(H_Z)\right]\right]$$
$$+\operatorname{vec}(\Gamma)^\top\mathbb{E}_{\boldsymbol{w}}\left[\mathbb{E}_{\boldsymbol{x},\epsilon}\left[\operatorname{vec}(H_Z)\operatorname{vec}(H_Z)^\top\right]\right]\operatorname{vec}(\Gamma) \tag{A.41}$$

where the difference between IDG and ICL error comes from the different task distribution over which we take $\mathbb{E}_{\boldsymbol{w}}$. Note this $\mathbb{E}_{\boldsymbol{w}}$ is shorthand for "expectation over task distribution," which will be different distributions depending on if we are using $\mathcal{P}_{\mathrm{IDG}}$ or $\mathcal{P}_{\mathrm{ICL}}$.

Now we can use the above Lemma to simplify these terms drastically. For the IDG distribution, we have

$$\mathbb{E}_{\boldsymbol{w}}[\boldsymbol{w}] = \boldsymbol{b}_k\,, \qquad \mathbb{E}_{\boldsymbol{w}}[\boldsymbol{w}\boldsymbol{w}^\top] = R_k\,.$$

Therefore,

$$\mathbb{E}_{\boldsymbol{w}}[\mathbb{E}_{\boldsymbol{x},\epsilon}[y_{\ell+1}^2]] = \mathrm{tr}[\Sigma R_k] + \rho \tag{A.42}$$

$$\mathbb{E}_{\boldsymbol{w}}[\mathbb{E}_{\boldsymbol{x},\epsilon}[y_{\ell+1}H_Z]] = \frac{1}{d}\left[\Sigma R_k\Sigma \quad (\mathrm{tr}[\Sigma R_k]+\rho)\,\Sigma\boldsymbol{b}_k\right] = \frac{1}{d}A_{\mathrm{IDG}} \tag{A.43}$$

$$\begin{aligned}\mathbb{E}_{\boldsymbol{x},\epsilon}[\mathrm{vec}(H_Z)\,\mathrm{vec}(H_Z)^\top] &\simeq \frac{1}{d}\Sigma\otimes\begin{bmatrix}\Sigma R_k\Sigma + \frac{d}{\ell}\,(\mathrm{tr}[\Sigma R_k]+\rho)\,\Sigma & (\mathrm{tr}[\Sigma R_k]+\rho)\,\Sigma\boldsymbol{b}_k \\ (\mathrm{tr}[\Sigma R_k]+\rho)\,(\Sigma\boldsymbol{b}_k)^\top & (\mathrm{tr}[\Sigma R_k]+\rho)^2\end{bmatrix} \\ &= \frac{1}{d}\Sigma\otimes B_{\mathrm{IDG}}\,.\end{aligned} \tag{A.44}$$

For the ICL distribution, we have

$$\mathbb{E}_{\boldsymbol{w}}[\boldsymbol{w}] = 0\,, \qquad \mathbb{E}_{\boldsymbol{w}}[\boldsymbol{w}\boldsymbol{w}^\top] = C_{\mathrm{test}}\,,$$

and so

$$\mathbb{E}_{\boldsymbol{w}}\left[\mathbb{E}_{\boldsymbol{x},\epsilon}[y_{\ell+1}^2]\right] = \mathbb{E}_{\boldsymbol{w}}\left[\mathrm{tr}[\Sigma\boldsymbol{w}\boldsymbol{w}^\top]+\rho\right] = \mathrm{tr}[\Sigma C_{\mathrm{test}}]+\rho \tag{A.45}$$

$$\mathbb{E}_{\boldsymbol{w}}\left[\mathbb{E}_{\boldsymbol{x},\epsilon}[y_{\ell+1}H_Z]\right] = \frac{1}{d}\left[\Sigma C_{\mathrm{test}}\Sigma \quad 0\right] = \frac{1}{d}A_{\mathrm{ICL}} \tag{A.46}$$

$$\begin{aligned}\mathbb{E}_{\boldsymbol{w}}\left[\mathbb{E}_{\boldsymbol{x},\epsilon}[\mathrm{vec}(H_Z)\,\mathrm{vec}(H_Z)^\top]\right] &\simeq \frac{1}{d}\Sigma\otimes\begin{bmatrix}\Sigma C_{\mathrm{test}}\Sigma + \frac{d}{\ell}\,(\mathrm{tr}[\Sigma C_{\mathrm{test}}]+\rho)\,\Sigma & 0 \\ 0^\top & (\mathrm{tr}[\Sigma C_{\mathrm{test}}]+\rho)^2\end{bmatrix} \\ &= \frac{1}{d}\Sigma\otimes B_{\mathrm{ICL}}\,.\end{aligned} \tag{A.47}$$

Upon noting that

$$\mathrm{vec}(\Gamma)^\top(\Sigma\otimes B)\,\mathrm{vec}(\Gamma) = \mathrm{tr}\left(\Sigma\Gamma B\Gamma^\top\right)\,,$$

substituting these components into (A.41) gives the required results. □

B Random Matrix Theory Calculation

Note that while Result 1 is offered for general token covariance Σ, all steps and results in this section and the following section assume $\Sigma = I_d$.

The setup and structure of this formalism and corresponding results will follow Section SI.3 and SI.4 of Lu et al. (2025). There will be key differences caused by the different task statistics $\mathcal{N}(0, C_{\mathrm{train}}), \mathcal{N}(0, C_{\mathrm{test}})$ that we use in this work compared to the isotropic tasks used in Lu et al. (2025). Since the token structure is the same between the work of Lu et al. (2025) and our work here, we will not prove various error bounding claims or approximations rigorously here, as such bounds would be identical to what can be found in Lu et al. (2025). However, care will be taken to highlight the distinction and differences required for handling the additional complexity introduced by our consideration of non-isotropic tasks.

We will use $\approx$ to denote two scalar quantities which converge in probability in the high-dimensional limit, or for two matrices to represent deterministic equivalence.

Definition 1. *For two $d \times d$ (possibly random) matrices A_d and B_d, we write $A_d \simeq B_d$ if $\mathrm{tr}[M_d(A_d - B_d)] \to 0$ in probability as $d \to \infty$ for any sequence of bounded spectral norm test matrices M_d (Atanasov et al., 2024; Lu et al., 2025).*

As noted above, we will not attempt to control rates of convergence.

We begin by considering the closed-form optimized parameters given by (11). This optimization problem can be solved explicitly as

$$\mathrm{vec}(\Gamma^*) = \left(\frac{n}{d}\lambda I + \sum_{\mu=1}^{n}\mathrm{vec}(H_{Z^\mu})\mathrm{vec}(H_{Z^\mu})^\top\right)^{-1}\sum_{\mu=1}^{n} y_{\ell+1}^{\mu}\mathrm{vec}(H_{Z^\mu})\,. \tag{B.1}$$

Ultimately we wish to characterize the ICL and IDG error of these parameters, which are given by Result 1 as

$$\mathcal{E}_{\rm ICL}(\Gamma^*) = \rho + \mathrm{tr}[C_{\rm test}] - 2\,\mathrm{tr}[\Gamma^* A_{\rm ICL}^\top] + \mathrm{tr}[\Gamma^* B_{\rm ICL}(\Gamma^*)^\top] \tag{B.2}$$

$$\mathcal{E}_{\rm IDG}(\Gamma^*) = \rho + \mathrm{tr}[R_k] - 2\,\mathrm{tr}[\Gamma^* A_{\rm IDG}^\top] + \mathrm{tr}[\Gamma^* B_{\rm IDG}(\Gamma^*)^\top] \tag{B.3}$$

for

$$A_{\rm ICL} = [C_{\rm test} \quad 0] \tag{B.4}$$

$$B_{\rm ICL} = \begin{bmatrix} C_{\rm test} + \frac{1}{\alpha_{\rm test}}(\mathrm{tr}[C_{\rm test}] + \rho) & 0 \\ 0^\top & (\mathrm{tr}[C_{\rm test}] + \rho)^2 \end{bmatrix} \tag{B.5}$$

$$A_{\rm IDG} = [R_k \quad (\mathrm{tr}[R_k] + \rho)\,\boldsymbol{b}_k] \tag{B.6}$$

$$B_{\rm IDG} = \begin{bmatrix} R_k + \frac{1}{\alpha_{\rm train}}(\mathrm{tr}[R_k] + \rho) & (\mathrm{tr}[R_k] + \rho)\,\boldsymbol{b}_k \\ (\mathrm{tr}[R_k] + \rho)\,\boldsymbol{b}_k^\top & (\mathrm{tr}[R_k] + \rho)^2 \end{bmatrix}. \tag{B.7}$$

Again, as we are distinguishing between pretraining and testing context lengths, we use

$$\alpha_{\rm train} = \ell_{\rm train}/d\,, \qquad \alpha_{\rm test} = \ell_{\rm test}/d\,.$$

These expressions for Γ^* and its corresponding errors depend explicitly on the randomness found in the particular sample of the data x, w, ϵ; we wish to be able to characterize the typical performance, and thus we need to average over this disorder. We will do so by following a random-matrix style computation that computes a deterministic equivalent for the parameter matrix Γ^* and its corresponding ICL and IDG errors, valid in high dimensions in the proportional limit

$$\frac{\ell_{\rm train}}{d} \equiv \alpha_{\rm train} = \Theta(1), \quad \frac{\ell_{\rm test}}{d} \equiv \alpha_{\rm test} = \Theta(1), \quad \frac{k}{d} \equiv \kappa = \Theta(1), \quad \frac{n}{d^2} \equiv \tau = \Theta(1). \tag{B.8}$$

To do this, we will express necessary quantities in terms of *resolvents.*

Resolvent and Extended Resolvent Setup

Γ^* above can be rewritten as

$$\mathrm{vec}(\Gamma^*) = G\left(\textstyle\sum_{\mu\in[n]} y_\mu\,\mathrm{vec}(H_\mu)\right)/d, \tag{B.9}$$

where G is the resolvent matrix

$$G = \left(\textstyle\sum_{\mu\in[n]} \mathrm{vec}(H_\mu)\,\mathrm{vec}(H_\mu)^\top/d + \tau\lambda I\right)^{-1}. \tag{B.10}$$

We will find it helpful to explicitly include an additional matrix $B_{\rm placeholder} \in \mathbb{R}^{(d^2+d)\times(d^2+d)}$ (that is positive-semidefinite)

$$G(\pi) = \left(\textstyle\sum_{\mu\in[n]} \mathrm{vec}(H_\mu)\,\mathrm{vec}(H_\mu)^\top/d + \pi B_{\rm placeholder} + \tau\lambda I\right)^{-1}, \tag{B.11}$$

for a non-negative scalar π. Notice that $G(0) = G$. Eventually $B_{\rm placeholder}$ will be explicitly related to $B_{\rm ICL}$ or $B_{\rm IDG}$ in a way that will allow us to more easily compute the $\Gamma B_{\rm ICL}\Gamma^\top$ or $\Gamma B_{\rm IDG}\Gamma^\top$ term in the error formulas.

We can write G in a cleaner and more useful way by concatenating y_μ and $\mathrm{vec}(H_\mu)$ into an extended vector

$$\boldsymbol{z}_\mu = \begin{bmatrix} y_\mu/d \\ \mathrm{vec}(H_\mu)/\sqrt{d} \end{bmatrix} \in \mathbb{R}^{d^2+d+1}. \tag{B.12}$$

We also extend $B_{\rm placeholder}$ as

$$B_{\rm ext} = \begin{bmatrix} 0 & \\ & B_{\rm placeholder} \end{bmatrix}, \tag{B.13}$$

We then define an extended resolvent (with very similar structure as G) to be

$$G_{\rm ext}(\pi) = \frac{1}{\sum_{\mu\in[n]} \boldsymbol{z}_\mu \boldsymbol{z}_\mu^\top + \pi B_{\rm ext} + \tau\lambda I}. \tag{B.14}$$

We see that $\boldsymbol{z}_\mu \boldsymbol{z}_\mu^\top$ and $B_{\rm ext}$ have block structure, and so expanding the block inverse we see

$$G_{\rm ext}(\pi) = \begin{bmatrix} c(\pi) & -c(\pi)q^\top(\pi) \\ -c(\pi)\boldsymbol{q}(\pi) & G(\pi) + c(\pi)\boldsymbol{q}(\pi)q^\top(\pi) \end{bmatrix}, \tag{B.15}$$

for

$$\boldsymbol{q}(\pi) \equiv \frac{1}{d^{3/2}} G(\pi) \left(\sum_{\mu \in [n]} y_\mu \operatorname{vec}(H_\mu) \right) \in \mathbb{R}^{d(d+1)} \tag{B.16}$$

and $c(\pi)$ defined self-consistently by

$$\frac{1}{c(\pi)} = \frac{1}{d^2} \sum_{\mu \in [n]} y_\mu^2 + \tau\lambda - \frac{1}{d^3} \sum_{\mu,\nu \in [n]} y_\mu y_\nu \operatorname{vec}(H_\mu)^\top G(\pi) \operatorname{vec}(H_\nu). \tag{B.17}$$

At $\pi = 0$ we can now see that G_{ext} explicitly contains information about the optimal parameters Γ^* we're considering, as

$$\boldsymbol{q}(0) = \frac{1}{\sqrt{d}} \operatorname{vec}(\Gamma^*) \,. \tag{B.18}$$

We will thus proceed by computing a deterministic equivalent for this extended resolvent.

Deterministic Equivalent for the Extended Resolvent

We will closely follow Reference Lu et al. (2025), omitting details that remain unchanged between the formalism in their work and ours here. Intuition-based headings will be given in *green*.

The computation proceeds by defining a "leave-one-out" version of G_{ext},

$$G_{\text{ext}}^{[\mu]} = \frac{1}{\sum_{\nu \neq \mu} \boldsymbol{z}_\nu \boldsymbol{z}_\nu^\top + \pi B_{\text{ext}} + \tau\lambda I}. \tag{B.19}$$

By construction,

$$G_{\text{ext}} \left(\sum_{\mu \in [n]} \boldsymbol{z}_\mu \boldsymbol{z}_\mu^\top + \pi B_{\text{ext}} + \tau\lambda I \right) = I. \tag{B.20}$$

$$\sum_{\mu \in [n]} \frac{1}{1 + \boldsymbol{z}_\mu^\top G_{\text{ext}}^{[\mu]} \boldsymbol{z}_\mu} G_{\text{ext}}^{[\mu]} \boldsymbol{z}_\mu \boldsymbol{z}_\mu^\top + G_{\text{ext}}(\pi B_{\text{ext}} + \tau\lambda I) = I. \tag{B.21}$$

Average over disorder in x, ϵ, which concentrates. The term $\boldsymbol{z}_\mu^\top G_{\text{ext}}^{[\mu]} \boldsymbol{z}_\mu$ is well-behaved, specifically as argued by Lu et al. (2025), it concentrates around its conditional expectation when the task $\boldsymbol{w}_\mu$ and $G_{\text{ext}}^{[\mu]}$ is fixed. We thus have

$$\boldsymbol{z}_\mu^\top G_{\text{ext}}^{[\mu]} \boldsymbol{z}_\mu \simeq \chi^\mu(\boldsymbol{w}_\mu) \tag{B.22}$$

where

$$\chi^\mu(\boldsymbol{w}_\mu) \equiv \frac{1}{d^2} \operatorname{tr} \left([G_{\text{ext}}^\mu]_{\setminus 0} \cdot [I \otimes E(\boldsymbol{w}_\mu)] \right), \tag{B.23}$$

and

$$E(\boldsymbol{w}) \equiv \begin{bmatrix} \boldsymbol{w}\boldsymbol{w}^\top + \frac{1}{\alpha} \left(\rho + \operatorname{tr}[\boldsymbol{w}\boldsymbol{w}^\top] \right) I_d & \left(\rho + \operatorname{tr}[\boldsymbol{w}\boldsymbol{w}^\top] \right) w \\ \left(\rho + \operatorname{tr}[\boldsymbol{w}\boldsymbol{w}^\top] \right) w^\top & \left(\rho + \operatorname{tr}[\boldsymbol{w}\boldsymbol{w}^\top] \right)^2 \end{bmatrix}. \tag{B.24}$$

Replacing $\boldsymbol{z}_\mu^\top G_{\text{ext}}^{[\mu]} \boldsymbol{z}_\mu$ in (B.21) with $\chi^\mu(\boldsymbol{w}_\mu)$ gives

$$\sum_{\mu \in [n]} \frac{1}{1 + \chi^\mu(\boldsymbol{w}_\mu)} G_{\text{ext}}^{[\mu]} \boldsymbol{z}_\mu \boldsymbol{z}_\mu^\top + G_{\text{ext}}(\pi B_{\text{ext}} + \tau\lambda I) \simeq I \,. \tag{B.25}$$

Next, we will also average the term $\boldsymbol{z}_\mu \boldsymbol{z}_\mu^\top$ on on the left-hand side of (B.25) over the remaining disorder in $\boldsymbol{x}, \epsilon$, holding $\boldsymbol{w}$ fixed, and replace $\boldsymbol{z}_\mu \boldsymbol{z}_\mu^\top$ with this conditional expectation. Doing so introduces some small error which is bounded in Lu et al. (2025). From this we have

$$\sum_{\mu \in [n]} \frac{1}{1 + \chi^\mu(\boldsymbol{w}_\mu)} G_{\text{ext}}^{[\mu]} \mathbb{E}_{\boldsymbol{x},\epsilon}[\boldsymbol{z}_\mu \boldsymbol{z}_\mu^\top] + G_{\text{ext}}(\pi B_{\text{ext}} + \tau\lambda I) \simeq I \,. \tag{B.26}$$

We already have enough to compute $\mathbb{E}_{\boldsymbol{x},\epsilon}[\boldsymbol{z}_\mu \boldsymbol{z}_\mu^\top]$ using Lemma 2 as

$$\mathbb{E}_{\boldsymbol{x},\epsilon}[\boldsymbol{z}_\mu \boldsymbol{z}_\mu^\top] \simeq \frac{1}{d^2} \Upsilon, \tag{B.27}$$

where because it will appear in subsequent equations we define the matrix

$$\Upsilon \equiv \begin{bmatrix} \rho + \operatorname{tr}[\boldsymbol{w}\boldsymbol{w}^\top] & \frac{1}{\sqrt{d}} \operatorname{vec}\left(\begin{bmatrix} \boldsymbol{w}\boldsymbol{w}^\top & (\rho + \operatorname{tr}[\boldsymbol{w}\boldsymbol{w}^\top])\boldsymbol{w} \end{bmatrix} \right)^\top \\ \frac{1}{\sqrt{d}} \operatorname{vec}\left(\begin{bmatrix} \boldsymbol{w}\boldsymbol{w}^\top & (\rho + \operatorname{tr}[\boldsymbol{w}\boldsymbol{w}^\top])\boldsymbol{w} \end{bmatrix} \right) & I_d \otimes E(\boldsymbol{w}) \end{bmatrix}. \tag{B.28}$$

Now substitute this expression into (B.26) for the conditional expectation $\mathbb{E}_{\boldsymbol{x},\epsilon}\left[\boldsymbol{z}_\mu \boldsymbol{z}_\mu^\top\right]$, giving

$$\frac{\tau}{n}\sum_{\mu\in[n]}\frac{1}{1+\chi^\mu(\boldsymbol{w}_\mu)}G_{\text{ext}}^{[\mu]}\Upsilon + G_{\text{ext}}(\pi B_{\text{ext}} + \tau\lambda I) \simeq I \tag{B.29}$$

where we recall $\tau = n/d^2$.

"Leave-one-out" terms behave like their full-sum equivalents. In high dimensions and for large n, there is negligible difference between $\sum_{\nu\neq\mu}$ and $\sum_\mu$. Thus, we replace G_{ext}^μ by G_{ext}, and $\chi^\mu(\boldsymbol{w}_\mu)$ by

$$\chi(\boldsymbol{w}_\mu) \equiv \frac{1}{d^2}\,\text{tr}\left([G_{\text{ext}}]_{\setminus 0}\cdot[I\otimes E(\boldsymbol{w}_\mu)]\right). \tag{B.30}$$

So finally we have the expression for G_{ext}

$$G_{\text{ext}}\left(\frac{\tau}{n}\sum_{\mu\in[n]}\frac{1}{1+\chi(\boldsymbol{w}_\mu)}\Upsilon + \pi B_{\text{ext}} + \tau\lambda I\right) \simeq I\,. \tag{B.31}$$

Exploit finiteness of training task set. So far we are summing over n task vectors, but really only n/k of these are unique. Thus, we can simplify (B.31) as

$$G_{\text{ext}}\left(\frac{\tau}{k}\sum_{j\in[k]}\frac{1}{1+\chi(\boldsymbol{t}_j)}\Upsilon + \pi B_{\text{ext}} + \tau\lambda I\right) \simeq I\,. \tag{B.32}$$

Indeed $\chi(\boldsymbol{t}_j)$ is also self-averaging in $\boldsymbol{t}_j$, and as argued by Lu et al. (2025), concentrates to its mean

$$\widehat{\chi}_{\text{ave}} \equiv \frac{1}{k}\sum_{j\in[k]}\chi(\boldsymbol{t}_j). \tag{B.33}$$

We can thus simplify our expressions by substituting (B.30) into (B.33) and performing the sum over $w_1, ..., w_k$. Here we will use the that

$$\frac{1}{k}\sum_{j\in[k]}\left(\rho + \text{tr}[\boldsymbol{t}_j\boldsymbol{t}_j^\top]\right) = \rho + \text{tr}[R_k] \tag{B.34}$$

$$\frac{1}{k}\sum_{j\in[k]}\left(\rho + \text{tr}[\boldsymbol{t}_j\boldsymbol{t}_j^\top]\right)\boldsymbol{t}_j \simeq (\rho + \text{tr}[R_k])\,\boldsymbol{b}_k \tag{B.35}$$

$$\frac{1}{k}\sum_{j\in[k]}\left(\rho + \text{tr}[\boldsymbol{t}_j\boldsymbol{t}_j^\top]\right)^2 \simeq (\rho + \text{tr}[R_k])^2 \tag{B.36}$$

where for (B.35) and (B.36) we have used that $\text{tr}[\boldsymbol{t}_j\boldsymbol{t}_j^\top] \simeq \text{tr}[R_k]$ as $\text{tr}[R_k] - \text{tr}[\boldsymbol{t}_j\boldsymbol{t}_j^\top]$ has mean 0 and variance $\Theta(1/d)$. We thus have that

$$\frac{1}{k}\sum_{j\in[k]}E(\boldsymbol{t}_j) \simeq B_{\text{IDG}} \tag{B.37}$$

and so

$$\widehat{\chi}_{\text{ave}} = \frac{1}{d^2}\,\text{tr}\left([G_{\text{ext}}]_{\setminus 0}\cdot[I\otimes B_{\text{IDG}}]\right). \tag{B.38}$$

Final formula for extended resolvent in terms of training task sample. The extended resolvent $G_{\text{ext}}(\pi)$ is asymptotically equivalent to

$$\widehat{\mathcal{G}}_e(\pi) \equiv \left(\frac{\tau}{1+\widehat{\chi}_{\text{ave}}}\begin{bmatrix}\rho_{\text{train}} & \frac{1}{\sqrt{d}}\,\text{vec}\left([R_k \quad \rho_{\text{train}}\boldsymbol{b}_k]\right)^\top \\ \frac{1}{\sqrt{d}}\,\text{vec}\left([R_k \quad \rho_{\text{train}}\boldsymbol{b}_k]\right) & I_d\otimes B_{\text{IDG}}\end{bmatrix} + \pi B_{\text{ext}} + \tau\lambda I\right)^{-1} \tag{B.39}$$

with $\widehat{\chi}_{\text{ave}}$ defined self-consistently by

$$\widehat{\chi}_{\text{ave}} \equiv \frac{1}{k}\sum_{j\in[k]}\chi(\boldsymbol{t}_j) = \frac{1}{d^2}\mathbb{E}\left[\text{tr}\left([G_{\text{ext}}]_{\setminus 0}\cdot[I_d\otimes B_{\text{IDG}}]\right)\right] \tag{B.40}$$

with

$$\boldsymbol{b}_k \equiv \frac{1}{k}\sum_{j\in[k]} \boldsymbol{t}_j\,, \qquad R_k \equiv \frac{1}{k}\sum_{j\in[k]} \boldsymbol{t}_j\boldsymbol{t}_j^\top\,, \qquad \rho_{\text{train}} \equiv \rho + \text{tr}[R_k]\,, \tag{B.41}$$

$$B_{\text{IDG}} \equiv \begin{bmatrix} R_k + \frac{\rho_{\text{train}}}{\alpha} I_d & \rho_{\text{train}}\boldsymbol{b}_k \\ \rho_{\text{train}}\boldsymbol{b}_k^\top & \rho_{\text{train}}^2 \end{bmatrix}. \tag{B.42}$$

Simplifying self-consistency variable χ. χ is defined in terms of the dominant component $[G_{\text{ext}}]_{\setminus 0}$ of G_{ext}. To simplify this, choose ansatz for B_{ext} as

$$B_{\text{ext}} = \begin{bmatrix} 0 & 0 \\ 0 & I_d \otimes B_{\text{test}} \end{bmatrix}$$

where B_{test} will later be B_{ICL} or B_{IDG} depending on which error we compute. Then $[G_{\text{ext}}]_{\setminus 0}$ can be expanded as

$$\begin{aligned} &\left(\frac{\tau}{1+\chi_\pi} I_d \otimes B_{\text{IDG}} + \pi I_d \otimes B_{\text{test}} + \tau\lambda I_d \otimes I_{d+1}\right)^{-1} \\ &= I_d \otimes \left(\frac{\tau}{1+\chi_\pi} B_{\text{IDG}} + \pi B_{\text{test}} + \tau\lambda I_{d+1}\right)^{-1} &\text{(B.43)} \\ &= I_d \otimes F_E(\pi) &\text{(B.44)} \end{aligned}$$

where

$$F_E(\pi) \equiv \left(\frac{\tau}{1+\chi_\pi} B_{\text{IDG}} + \pi B_{\text{test}} + \tau\lambda I_{d+1}\right)^{-1}.$$

We can use this to replace $\widehat{\chi}_{\text{ave}}$ with χ_π defined self-consistently by

$$\chi_\pi \simeq \frac{1}{d}\,\text{tr}\left[\left(\frac{\tau}{1+\chi_\pi} B_{\text{IDG}} + \pi B_{\text{test}} + \lambda\tau I_{d+1}\right)^{-1} B_{\text{IDG}}\right] \tag{B.45}$$

Relating $\widehat{\mathcal{G}}_e(\pi)$ to a deterministic equivalent for Γ^*. Lu et al. (2025) shows that two key quantities $\text{tr}[\Gamma^* A^\top]$ and $\text{tr}[\Gamma^* B(\Gamma^*)^\top]$ in $\mathcal{E}(\Gamma^*)$ can also be computed from the extended resolvent $G_{\text{ext}}(\pi)$. As this is purely a matrix algebra claim, and independent of the particular task structure hidden within Γ^*, it generalizes immediately to our case. We thus include this result here without proof and refer to reader to Lu et al. (2025) for a derivation.

Lemma 3. ***[From Lu et al. (2025)]*** *For any matrix $A \in \mathbb{R}^{d\times(d+1)}$,*

$$\text{tr}[\Gamma^* A^\top] = \frac{-1}{c(0)\sqrt{d}} \begin{bmatrix} 0 & \text{vec}(A)^T \end{bmatrix} G_{\text{ext}}(0)\boldsymbol{e}_1, \tag{B.46}$$

where $\boldsymbol{e}_1$ denotes the first natural basis vector in $\mathbb{R}^{d^2+d+1}$. For any symmetric and positive semidefinite matrix $B \in \mathbb{R}^{(d+1)\times(d+1)}$, if we set

$$B_{\text{placeholder}} = I_d \otimes B \tag{B.47}$$

in (B.13), then

$$\text{tr}[\Gamma^* B(\Gamma^*)^\top] = \frac{d}{d\pi}\left(\frac{1}{c(\pi)}\right)\Big|_{\pi=0}. \tag{B.48}$$

Using Lemma 3, we can find the deterministic equivalent for Γ^* from

$$\begin{aligned} \text{tr}[\Gamma^* A^\top] &\simeq \frac{-1}{c(0)\sqrt{d}} \begin{bmatrix} 0 & \text{vec}(A)^T \end{bmatrix} \mathcal{G}_e(0)\boldsymbol{e}_1 &\text{(B.49)} \\ &= \frac{c^*(0)}{c(0)} \cdot \frac{1}{d}\,\text{tr}\left(\begin{bmatrix} R_k & \rho_{\text{train}}\boldsymbol{b}_k \end{bmatrix} (B_{\text{IDG}} + \lambda(1+\chi_0)I)^{-1} A^\top\right) &\text{(B.50)} \\ &\simeq \frac{1}{d}\,\text{tr}\left(\begin{bmatrix} R_k & \rho_{\text{train}}\boldsymbol{b}_k \end{bmatrix} (B_{\text{IDG}} + \lambda(1+\chi_0)I)^{-1} A^\top\right). &\text{(B.51)} \end{aligned}$$

and thus

$$\Gamma^*_{\text{eq}} \simeq \begin{bmatrix} R_k & \rho_{\text{train}}\boldsymbol{b}_k \end{bmatrix} (B_{\text{IDG}} + \lambda(1+\chi_0)I)^{-1} \tag{B.52}$$

SELF-CONSISTENCY EQUATIONS AND FINITE TASK SAMPLE AVERAGES

So far, everything is left in terms of the quantities $\boldsymbol{b}_k, R_k, B_{\text{IDG}}$ that depend on a typical sample of k task vectors $w_1, \cdots, w_k$. What remains to be analyzed is the behavior of this sample and its sample statistics, *i.e.*, how does the finiteness of k affect Γ^*. The following steps will deal with this.

Characterization of χ_0 We see that we almost have a characterization for the deterministic equivalent of Γ^* but we need to understand what $\lambda(1+\chi_0)$ term is doing. From (B.45) we know χ_0 is defined self-consistently from

$$\chi_0 \simeq \frac{1}{d}\operatorname{tr}\left[\left(\frac{\tau}{1+\chi_0}B_{\text{IDG}} + \lambda\tau I_{d+1}\right)^{-1} B_{\text{IDG}}\right] \tag{B.53}$$

$$\frac{\tau\chi_0}{1+\chi_0} \simeq \frac{1}{d}\operatorname{tr}\left[\left(B_{\text{IDG}} + \lambda(1+\chi_0)I_{d+1}\right)^{-1} B_{\text{IDG}}\right] \tag{B.54}$$

$$= \frac{d+1}{d} - \lambda(1+\chi_0)\frac{1}{d}\operatorname{tr}\left[\left(B_{\text{IDG}} + \lambda(1+\chi_0)I_{d+1}\right)^{-1}\right] \tag{B.55}$$

Remember B_{IDG} is a $(d+1)\times(d+1)$ block matrix with upper $d\times d$ block given by $R_k + \rho_{\text{train}}/\alpha$. We wish to express the above resolvent just in terms of R_k.

Working heuristically and block-inverting the $B_{\text{IDG}} + \lambda(1+\chi)$ resolvent we have

$$\frac{1}{d}\operatorname{tr}\left[\left(B_{\text{IDG}} + \lambda(1+\chi_0)I_{d+1}\right)^{-1}\right] \simeq \frac{1}{d}\operatorname{tr}(F_R(\sigma)) \tag{B.56}$$

where

$$\sigma \equiv \frac{\rho_{\text{train}}}{\alpha} + \lambda(1+\chi_0) \tag{B.57}$$

$$F_R(\sigma) \equiv (R_k + \sigma I_d)^{-1} \tag{B.58}$$

Sample covariance R_k and the Stieltjes transform. We thus have

$$\frac{\tau\chi_0}{1+\chi_0} \simeq \frac{d+1}{d} - \lambda(1+\chi_0)\frac{1}{d}\operatorname{tr}[F_R(\sigma_0)] \simeq 1 - \lambda(1+\chi_0)\mathcal{M}_\kappa\left(\frac{\rho_{\text{train}}}{\alpha} + \lambda(1+\chi_0)\right)$$

where $\mathcal{M}_\kappa(\sigma)$ is the asymptotic equivalent of the Stieltjies transform of the Wishart resolvent

$$F_R(\sigma) = (R_k + \sigma I_d)^{-1}.$$

Following Atanasov et al. (2024) for correlated feature wisharts, we have

$$\mathcal{M}_\kappa(\sigma) = \frac{1}{d}s\operatorname{tr}((C_{\text{train}} + s\sigma\mathbb{I})^{-1}) \tag{B.59}$$

where s is defined by the self consistency equation

$$\frac{1}{s} = 1 - \frac{1}{\kappa}\frac{1}{d}\operatorname{tr}(C_{\text{train}}(C_{\text{train}} + s\sigma\mathbb{I})^{-1}) = 1 - \frac{1}{\kappa} + \frac{\sigma}{\kappa}\mathcal{M}_\kappa(\sigma) \tag{B.60}$$

and also only depends on σ, κ, and C_{train}. In other words, we have a self-consistency equation for $\mathcal{M}_\kappa(\sigma)$ as

$$\mathcal{M}_\kappa(\sigma) = \operatorname{tr}\left[\left(\left(1 - \frac{1}{\kappa} + \frac{\sigma}{\kappa}\mathcal{M}_\kappa(\sigma)\right)C_{\text{train}} + \sigma I_d\right)^{-1}\right]. \tag{B.61}$$

Similarly, we can express F_R in deterministic form as

$$(R_k + \sigma I_d)^{-1} \simeq F_\kappa(\sigma) \equiv \left(\left(1 - \frac{1}{\kappa} + \frac{\sigma}{\kappa}\mathcal{M}_\kappa(\sigma)\right)C_{\text{train}} + \sigma I_d\right)^{-1}. \tag{B.62}$$

Note that

$$(R_k + \sigma I_d)^{-2} \simeq -\frac{\mathrm{d}}{\mathrm{d}\sigma}F_\kappa(\sigma) = -F_\kappa(\sigma)\left(\left(\frac{1}{\kappa}\mathcal{M}_\kappa(\sigma) + \frac{\sigma}{\kappa}\frac{\mathrm{d}}{\mathrm{d}\sigma}\mathcal{M}_\kappa(\sigma)\right)C_{\text{train}} + I_d\right)F_\kappa(\sigma). \tag{B.63}$$

Given a particular problem with a particular C_{train}, each of these can be computed.

Self-Consistency equation for χ_0 Recall to characterize Γ^*_{eq} we need to understand $\lambda(1+\chi_0) \equiv \tilde{\lambda}$. We now know this variable is defined by

$$\tilde{\lambda}\mathcal{M}_\kappa\left(\frac{\rho_{\text{train}}}{\alpha}+\tilde{\lambda}\right)-\frac{\lambda\tau}{\tilde{\lambda}}=1-\tau \tag{B.64}$$

In the ridgeless $\lambda \to 0$ limit this equation becomes

$$\tilde{\lambda}\mathcal{M}_\kappa\left(\frac{\rho_{\text{train}}}{\alpha}+\tilde{\lambda}\right)=1-\tau\,. \tag{B.65}$$

While this equation has nontrivial solutions for $\tau < 1$, it's only solution is $\tilde{\lambda} = 0$ when $\tau > 1$.

Final deterministic equivalence for Γ^* in terms of Wishart resolvent. Recall from above that

$$\Gamma^*_{\text{eq}} = (B_{\text{IDG}} + \hat{\lambda}\, I_{d+1})^{-1}[R_k \quad \rho_{\text{train}}\boldsymbol{b}_k]$$

We can use the trick that

$$[R_k \quad \rho_{\text{train}}\boldsymbol{b}_k] = S\left(B_{\text{IDG}} + \tilde{\lambda}_C I_{d+1} - \left(\frac{\rho_{\text{train}}}{\alpha}+\tilde{\lambda}_C\right)I_{d+1}\right) \tag{B.66}$$

where S is an almost-identity matrix that selects top $d \times (d+1)$ of a $(d+1)\times(d+1)$ matrix. We can then simplify

$$\Gamma^*_{\text{eq}} = S\left(I - \left(\frac{\rho_{\text{train}}}{\alpha}+\tilde{\lambda}\right)(B_{\text{IDG}}+\tilde{\lambda}I)^{-1}\right) \tag{B.67}$$

$$\simeq [I - \sigma F_R(\sigma) \quad 0]\,. \tag{B.68}$$

We stress that this is an approximation that comes from the full block inversion of the resolvent of B_{IDG}, but is robustly handled in Lu et al. (2025).

Characterization of Quadratic term in error.

The only remaining error term left to approximate is those with the form $\Gamma B \Gamma^\top$. This is what we introduced π and B_{ext} for.

$$\frac{1}{d}\operatorname{tr}\left(I_d \Gamma B_{\text{test}} \Gamma^\top\right) = \frac{1}{d}\operatorname{vec}(\Gamma)^\top \Pi \operatorname{vec}(\Gamma) = \frac{\mathrm{d}}{\mathrm{d}\pi}\frac{1}{c(\pi)}(\pi = 0) \tag{B.69}$$

for $B_{\text{placeholder}} = I_d \otimes B_{\text{test}}$. The definition of $c(\pi)$ comes from the scalar term in the block inversion of $G_{\text{ext}}(\pi)$,

$$\mathcal{G}_e(\pi) = \begin{bmatrix} c^*(\pi) & -c^*(\pi)\,(\boldsymbol{q}^*(\pi))^\top \\ -c^*(\pi)\,\boldsymbol{q}^*(\pi) & I \otimes F_E(\chi_\pi) + c^*(\pi)\boldsymbol{q}^*(\pi)(\boldsymbol{q}^*(\pi))^\top \end{bmatrix}, \tag{B.70}$$

with

$$\frac{1}{c^*(\pi)} = \frac{\tau\rho_{\text{train}}}{1+\chi_\pi} + \lambda\tau - \frac{\tau^2}{(1+\chi_\pi)^2}\frac{1}{d}\operatorname{tr}\left([R_k \quad \rho_{\text{train}}\boldsymbol{b}_k]\, F_E(\chi_\pi)\, [R_k \quad \rho_{\text{train}}\boldsymbol{b}_k]^\top\right). \tag{B.71}$$

with

$$\chi_\pi \simeq \frac{1}{d}\operatorname{tr}\left[\left(\frac{\tau}{1+\chi_\pi}B_{\text{IDG}} + \pi B + \lambda\tau I_{d+1}\right)^{-1} B_{\text{IDG}}\right] \tag{B.72}$$

$$F_E(\chi_\pi) = \left(\frac{\tau}{1+\chi_\pi}B_{\text{IDG}} + \pi B_{\text{test}} + \tau\lambda I_{d+1}\right)^{-1} \tag{B.73}$$

Now following through the calculus, we get

$$\frac{\mathrm{d}}{\mathrm{d}\pi}F_E(\chi_\pi) = -F_E(\chi_\pi)\left(B_{\text{test}} - \frac{\tau}{(1+\chi_\pi)^2}\left(\frac{\mathrm{d}}{\mathrm{d}\pi}\chi_\pi\right)B_{\text{IDG}}\right)F_E(\chi_\pi) \tag{B.74}$$

$$\frac{\mathrm{d}}{\mathrm{d}\pi}\chi_\pi = \frac{1}{d}\operatorname{tr}\left[\left(\frac{\mathrm{d}}{\mathrm{d}\pi}F_E(\chi_\pi)\right)B_{\text{IDG}}\right] \tag{B.75}$$

Plugging (B.74) into (B.75) and simplifying for χ_0' gives

$$\frac{\tau\chi_0'}{(1+\chi_0)^2} = \frac{\frac{1}{d}\operatorname{tr}\left(B_{\text{test}}F_0 B_{\text{IDG}} F_0\right)}{\frac{1}{d}\operatorname{tr}(F_0 B_{\text{IDG}} F_0 B_{\text{IDG}}) - \tau} = \frac{\frac{1}{d}\operatorname{tr}(B_{\text{test}}F_0) - \tilde{\lambda}\frac{1}{d}\operatorname{tr}(B_{\text{test}}F_0^2)}{1 - 2\tilde{\lambda}\frac{1}{d}\operatorname{tr}(F_0) + \tilde{\lambda}^2\frac{1}{d}\operatorname{tr}(F_0^2) - \tau} \tag{B.76}$$

for

$$F_0 \equiv \left(B_{\text{IDG}} + \tilde{\lambda} I_{d+1}\right)^{-1}, \qquad \tilde{\lambda} \equiv \lambda(1+\chi_0)\,.$$

We can finally simplify the quadratic term as

$$\left(\frac{\mathrm{d}}{\mathrm{d}\pi}\frac{1}{c(\pi)}\right)(\pi=0) = \frac{1}{d}\operatorname{tr}(\Gamma^*_{\mathrm{eq}} B_{\mathrm{test}} \Gamma^*_{\mathrm{eq}}) - \tau\frac{\chi_0'}{(1+\chi_0)^2}\left(\rho_{\mathrm{train}} - \frac{1}{d}\operatorname{tr}(\Gamma^*_{\mathrm{eq}} A_{\mathrm{IDG}}^\top) - \tilde{\lambda}\frac{1}{d}\operatorname{tr}(\Gamma^*_{\mathrm{eq}}(\Gamma^*_{\mathrm{eq}})^\top)\right) \tag{B.77}$$

Dictionary of various deterministic equivalents

Lemma 4. *The following is a summary of formulas. Their derivations follow simply from the above discussions and characterizations. Let*

$$F_0 \equiv \left(B_{IDG} + \tilde{\lambda} I_{d+1}\right)^{-1}, \qquad \tilde{\lambda} \equiv \lambda(1+\chi_0)$$

and Γ^*_{eq} *as given by (B.68). Then*

$$\operatorname{tr}[F_0(\tilde{\lambda})] \simeq \mathcal{M}_\kappa(\sigma) \tag{B.78}$$

$$\operatorname{tr}[F_0^2(\tilde{\lambda})] \simeq -\mathcal{M}_\kappa'(\sigma) \tag{B.79}$$

$$\operatorname{tr}[\Gamma^*_{\mathrm{eq}} A_{\mathrm{IDG}}^T] \simeq \operatorname{tr}[C_{\mathrm{train}}] - \sigma + \sigma^2\mathcal{M}_\kappa(\sigma) \tag{B.80}$$

$$\tilde{\lambda}\operatorname{tr}[\Gamma^*_{\mathrm{eq}}(\Gamma^*_{\mathrm{eq}})^\top] \simeq \tilde{\lambda}\left(1 - 2\sigma\mathcal{M}_\kappa(\sigma) - \sigma^2\mathcal{M}_\kappa'(\sigma)\right) \tag{B.81}$$

$$\operatorname{tr}[\Gamma^*_{\mathrm{eq}} A_{\mathrm{ICL}}^\top] \simeq \operatorname{tr}[C_{\mathrm{test}}] - \sigma\operatorname{tr}[F_\kappa(\sigma) C_{\mathrm{test}}] \tag{B.82}$$

$$\operatorname{tr}[B_{\mathrm{IDG}} F_0] = 1 - \tilde{\lambda}\mathcal{M}_\kappa(\sigma) \tag{B.83}$$

$$\operatorname{tr}[B_{\mathrm{IDG}} F_0^2] = \mathcal{M}_\kappa(\sigma) + \tilde{\lambda}\mathcal{M}_\kappa'(\sigma) \tag{B.84}$$

$$\operatorname{tr}[B_{\mathrm{ICL}} F_0] \simeq \operatorname{tr}\left[\left(C_{\mathrm{test}} + \frac{\rho_{\mathrm{test}}}{\alpha_{\mathrm{test}}} I_d\right) F_\kappa(\sigma)\right] \tag{B.85}$$

$$\operatorname{tr}[B_{\mathrm{ICL}} F_0^2] \simeq -\operatorname{tr}\left[\left(C_{\mathrm{test}} + \frac{\rho_{\mathrm{test}}}{\alpha_{\mathrm{test}}} I_d\right) F_\kappa'(\sigma)\right] \tag{B.86}$$

$$\operatorname{tr}[\Gamma^*_{\mathrm{eq}} B_{\mathrm{IDG}}(\Gamma^*_{\mathrm{eq}})^\top] \simeq \operatorname{tr}[\Gamma^*_{\mathrm{eq}} A_{\mathrm{IDG}}^\top] - \tilde{\lambda}\operatorname{tr}[\Gamma^*_{\mathrm{eq}}(\Gamma^*_{\mathrm{eq}})^\top] \tag{B.87}$$

$$\operatorname{tr}[\Gamma^*_{\mathrm{eq}} B_{\mathrm{ICL}}(\Gamma^*_{\mathrm{eq}})^\top] \simeq \operatorname{tr}\left[\left(C_{\mathrm{test}} + \frac{\rho_{\mathrm{test}}}{\alpha_{\mathrm{test}}} I_d\right)\left(I_d - 2\sigma F_\kappa(\sigma) - \sigma^2 F_\kappa'(\sigma)\right)\right] \tag{B.88}$$

C Proofs of Asympotic IDG and ICL Error Characterization

We finally have all the necessary components to write down the deterministic equivalents of the IDG and ICL errors given by Lemma 1 (or (B.3) and (B.2)). This will comprise our main theoretical result.

Result: High-dimensional formula for the IDG error

For $\mathcal{M}_\kappa(\sigma), \mathcal{M}_\kappa'(\sigma), \tilde{\lambda}$, and σ defined above, we have the deterministic equivalent of (A.2) as

$$\mathcal{E}_{\mathrm{IDG}}(\Gamma^*) \simeq \tau\frac{\rho + \sigma - \sigma^2\mathcal{M}_\kappa(\sigma) - \tilde{\lambda}(1 - 2\sigma\mathcal{M}_\kappa(\sigma) - \sigma^2\mathcal{M}_\kappa'(\sigma))}{\tau - (1 - 2\tilde{\lambda}\mathcal{M}_\kappa(\sigma) - \tilde{\lambda}^2\mathcal{M}_\kappa'(\sigma))} \equiv e_{\mathrm{IDG}}(C_{\mathrm{train}}) \tag{C.1}$$

Result: High-dimensional formula for the ICL error

Take $\mathcal{M}_\kappa(\sigma), \mathcal{M}'_\kappa(\sigma), F, F', \sigma$, and $\tilde{\lambda}$ as defined as above, and $q \equiv \mathcal{E}_{\text{IDG}}(\Gamma^*)/\tau$. The deterministic equivalent of (A.3) is then

$$\begin{aligned}\mathcal{E}_{\text{ICL}}(\Gamma^*) \simeq \rho + \frac{\rho + c_{\text{test}}}{\alpha_{\text{test}}} \Big(1 + (q - 2\sigma)\mathcal{M}_\kappa(\sigma) + (q\tilde{\lambda} - \sigma^2)\mathcal{M}'_\kappa(\sigma)\Big) \\ + \; q \operatorname{tr}\left[C_{\text{test}} F_\kappa(\sigma)\right] + (q\tilde{\lambda} - \sigma^2) \operatorname{tr}\left[C_{\text{test}} F'_\kappa(\sigma)\right] \\ \equiv e_{\text{ICL}}(C_{\text{train}}, C_{\text{test}})\,.\end{aligned} \tag{C.2}$$

Proof. Using Lemma 4 and (B.77) in (B.3) gives deterministic equivalent for $\mathcal{E}_{\text{IDG}}(\Gamma^*)$ as

$$\begin{aligned}\mathcal{E}_{\text{IDG}}(\Gamma^*) \simeq \rho + c_{\text{train}} - 2(c_{\text{train}} + \sigma + \sigma^2\mathcal{M}_\kappa(\sigma)) + c_{\text{train}} + \sigma \\ + \sigma^2\mathcal{M}_\kappa(\sigma) - \tilde{\lambda}(1 - 2\sigma\mathcal{M}_\kappa(\sigma) - \sigma^2\mathcal{M}'_\kappa(\sigma)) \\ - \frac{1 - 2\tilde{\lambda}\mathcal{M}_\kappa(\sigma) - \tilde{\lambda}^2\mathcal{M}'_\kappa(\sigma)}{-\tau + 1 - 2\tilde{\lambda}\mathcal{M}_\kappa(\sigma) - \tilde{\lambda}^2\mathcal{M}'_\kappa(\sigma)} \\ \times \Big(\rho_{\text{train}} - (c_{\text{train}} + \sigma + \sigma^2\mathcal{M}_\kappa(\sigma)) - \tilde{\lambda}(1 - 2\sigma\mathcal{M}_\kappa(\sigma) - \sigma^2\mathcal{M}'_\kappa(\sigma))\Big)\end{aligned} \tag{C.3}$$

$$\begin{aligned}= \Big(\rho - \sigma - \sigma^2\mathcal{M}_\kappa(\sigma) - \tilde{\lambda}(1 - 2\sigma\mathcal{M}_\kappa(\sigma) - \sigma^2\mathcal{M}'_\kappa(\sigma))\Big) \\ \times \left(1 - \frac{1 - 2\tilde{\lambda}\mathcal{M}_\kappa(\sigma) - \tilde{\lambda}^2\mathcal{M}'_\kappa(\sigma)}{-\tau + 1 - 2\tilde{\lambda}\mathcal{M}_\kappa(\sigma) - \tilde{\lambda}^2\mathcal{M}'_\kappa(\sigma)}\right)\end{aligned} \tag{C.4}$$

$$= \tau \frac{\rho - \sigma - \sigma^2\mathcal{M}_\kappa(\sigma) - \tilde{\lambda}(1 - 2\sigma\mathcal{M}_\kappa(\sigma) - \sigma^2\mathcal{M}'_\kappa(\sigma))}{\tau - (1 - 2\tilde{\lambda}\mathcal{M}_\kappa(\sigma) - \tilde{\lambda}^2\mathcal{M}'_\kappa(\sigma))} \tag{C.5}$$

as required.

Using Lemma 4 and (B.77) in (B.2) gives

$$\mathcal{E}_{\text{ICL}}(\Gamma^*) \simeq \quad \rho + c_{\text{test}} \tag{C.6}$$

$$- 2\left(c_{\text{test}} - \sigma \operatorname{tr}\left[C_{\text{test}} F_\kappa(\sigma)\right]\right) \tag{C.7}$$

$$+ \operatorname{tr}\left[\left(C_{\text{test}} + \frac{\rho + c_{\text{test}}}{\alpha_{\text{test}}} I_d\right)\left(I_d - 2\sigma F_\kappa(\sigma) - \sigma^2 F'_\kappa(\sigma)\right)\right] \tag{C.8}$$

$$+ \operatorname{tr}\left[\left(C_{\text{test}} + \frac{\rho + c_{\text{test}}}{\alpha_{\text{test}}} I_d\right)\left(F_\kappa(\sigma) + \tilde{\lambda} F'_\kappa(\sigma)\right)\right] \times \frac{\rho + \sigma - \sigma^2\mathcal{M}_\kappa(\sigma) - \tilde{\lambda}(1 - 2\sigma\mathcal{M}_\kappa(\sigma) - \sigma^2\mathcal{M}'_\kappa(\sigma))}{\tau - (1 - 2\tilde{\lambda}\mathcal{M}_\kappa(\sigma) - \tilde{\lambda}^2\mathcal{M}'_\kappa(\sigma))}\,. \tag{C.9}$$

Replacing

$$q \equiv \frac{\rho + \sigma - \sigma^2\mathcal{M}_\kappa(\sigma) - \tilde{\lambda}(1 - 2\sigma\mathcal{M}_\kappa(\sigma) - \sigma^2\mathcal{M}'_\kappa(\sigma))}{\tau - (1 - 2\tilde{\lambda}\mathcal{M}_\kappa(\sigma) - \tilde{\lambda}^2\mathcal{M}'_\kappa(\sigma))} \tag{C.10}$$

and gathering C_{test} terms we get

$$\begin{aligned}e_{\text{ICL}}(C_{\text{train}}, C_{\text{test}}) \simeq \rho + \frac{\rho + c_{\text{test}}}{\alpha_{\text{test}}} \Big(1 + (q - 2\sigma)\mathcal{M}_\kappa(\sigma) + (q\tilde{\lambda} - \sigma^2)\mathcal{M}'_\kappa(\sigma)\Big) \\ + \left\langle C_{\text{test}}, qF_\kappa(\sigma) + (q\tilde{\lambda} - \sigma^2)F'_\kappa(\sigma)\right\rangle\end{aligned} \tag{C.11}$$

as required. The remaining terms only depending on the test distribution through c_{test}, and thus not containing any structural information about the testing tasks, we call

$$e_{\text{scalar}}(\boldsymbol{\lambda}_{\text{train}}, c_{\text{test}}) \equiv \rho + \frac{\rho + c_{\text{test}}}{\alpha_{\text{test}}} \Big(1 + (q - 2\sigma)\mathcal{M}_\kappa(\sigma) + (q\tilde{\lambda} - \sigma^2)\mathcal{M}'_\kappa(\sigma)\Big) \tag{C.12}$$

and the remaining C_{test}-dependent terms form the $e_{\text{misalign}}(C_{\text{train}}, C_{\text{test}})$ contribution. □

D ORDERING OF EIGENVALUES

Here we analyze the spectrum of the C_{train}-dependent component of the misalignment error term (19),

$$\mathcal{K} \equiv qF_\kappa(\sigma) + (q\tilde{\lambda} - \sigma^2)F'_\kappa(\sigma)\,.$$

Given the self-consistent definitions of $F_\kappa(\sigma)$ and $F'_\kappa(\sigma)$ in (15) and (B.63), we can write the eigenvalues of $\mathcal{K}$ as

$$\lambda_i(\mathcal{K}) = \frac{1}{A_\kappa\lambda_i(C_{\text{train}}) + \sigma}\left(q + (\sigma^2 - q\tilde{\lambda})\frac{B_\kappa\lambda_i(C_{\text{train}}) + 1}{A_\kappa\lambda_i(C_{\text{train}}) + \sigma}\right)\,,$$

for

$$A_\kappa \equiv 1 - \frac{1}{\kappa} + \frac{\sigma}{\kappa}\mathcal{M}_\kappa(\sigma) \tag{D.1}$$

$$B_\kappa \equiv \frac{1}{\kappa}\mathcal{M}_\kappa(\sigma) + \frac{\sigma}{\kappa}\mathcal{M}'_\kappa(\sigma)\,. \tag{D.2}$$

Claim: Eigenvalue Ordering

We wish to show that

$$\lambda_1(\mathcal{K}) < \lambda_2(\mathcal{K}) < \cdots < \lambda_d(\mathcal{K})$$

for

$$\lambda_1(C_{\text{train}}) > \lambda_2(C_{\text{train}}) > \cdots > \lambda_d(C_{\text{train}})\,,$$

i.e. the ordering of eigenvalues of $\mathcal{K}$ is opposite that of C_{train}.

We will separate this into two cases. For $\tau > 1$ we provide a rigorous proof. For $\tau < 1$, due to the unclear sign of $\nu^2 - q\tilde{\lambda}$ we cannot currently provide a rigorous proof with the same methodology. Instead, we provide numerical plots supporting our claim, with the goal of proving this formally for the $\tau < 1$ case in subsequent iterations of this work.

Lemma. *We have that* $1 - \kappa \leq \sigma\mathcal{M}_\kappa(\sigma) \leq 1$ *and* $\sigma^2\mathcal{M}'_\kappa(\sigma) \leq \kappa - 1$.

Proof. R_k is a positive semi-definite matrix and so $\sigma(R_k + \sigma I_d)^{-1}$ is an increasing function of σ. Therefore $\sigma\,\text{tr}[(R_k + \sigma I_d)^{-1}]$ is increasing in σ and so

$$\lim_{d\to\infty} \sigma\,\text{tr}[(R_k + \sigma I_d)^{-1}] = \sigma\mathcal{M}_\kappa(\sigma)$$

is an increasing function of σ. Thus we have

$$\lim_{\sigma\to 0} \sigma\mathcal{M}_\kappa(\sigma) \leq \sigma\mathcal{M}_\kappa(\sigma).$$

Also as R_k is positive definite it is obvious that

$$\sigma\mathcal{M}_\kappa(\sigma) = \lim_{d\to\infty} \sigma\,\text{tr}[(R_k + \sigma I_d)^{-1}] \leq 1.$$

By an equivalent argument,

$$\sigma^2\mathcal{M}'_\kappa(\sigma) \leq \lim_{\sigma\to 0} \sigma^2\mathcal{M}'_\kappa(\sigma)\,.$$

It's helpful to first write the self-consistency equation

$$\mathcal{M}_\kappa(\sigma) = \text{tr}\left[\left(\left(1 - \frac{1}{\kappa} + \frac{\sigma}{\kappa}\mathcal{M}_\kappa(\sigma)\right)C_{\text{train}} + \sigma I_d\right)^{-1}\right] \tag{D.3}$$

for $\mathcal{M}_\kappa(\sigma)$ equivalently as a self-consistency equation for the "renormalized ridge" $\tilde{\sigma}$ of this Wishart resolvent, defined by

$$\tilde{\sigma}\,\text{tr}[(C_{\text{train}} + \tilde{\sigma})^{-1}] = \sigma\mathcal{M}_\kappa(\sigma)$$

or equivalently

$$\tilde{\sigma} = \frac{\sigma}{1 - \frac{1}{\kappa} + \frac{\tilde{\sigma}}{\kappa}\,\text{tr}\left[(C_{\text{train}} + \tilde{\sigma})^{-1}\right]}\,. \tag{D.4}$$

In the $\sigma \to 0$ limit, $\tilde{\sigma}$ limits to 0 when $\kappa > 1$, and limits to the unique solution of

$$1 - \frac{1}{\kappa} + \frac{\tilde{\sigma}}{\kappa}\,\text{tr}\left[(C_{\text{train}} + \tilde{\sigma})^{-1}\right] = 0 \tag{D.5}$$

for $\kappa < 1$. For our purposes, this means that

$$\lim_{\sigma \to 0} \sigma \mathcal{M}_\kappa(\sigma) = \begin{cases} 1-\kappa\,, & \kappa < 1 \\ 0\,, & \kappa > 1 \end{cases}. \tag{D.6}$$

Differentiating with respect to σ gives

$$\begin{aligned} \lim_{\sigma \to 0} \sigma^2 \mathcal{M}'_\kappa(\sigma) &= \begin{cases} \kappa - 1\,, & \kappa < 1 \\ 0\,, & \kappa > 1 \end{cases} \\ &\leq \kappa - 1 \end{aligned} \tag{D.7}$$

and so $1 - \kappa \leq \sigma \mathcal{M}_\kappa(\sigma)$ and $\sigma^2 \mathcal{M}'_\kappa(\sigma) \leq \kappa - 1$. □

For $\tau > 1$, have $\tilde{\lambda} = 0$ and so $\sigma = (\rho + c_{\text{train}})/\alpha$ and

$$\lambda_i(\mathcal{K}) = \frac{1}{A_\kappa \lambda_i(C_{\text{train}}) + \sigma} \left(q + \sigma^2 \frac{B_\kappa \lambda_i(C_{\text{train}}) + 1}{A_\kappa \lambda_i(C_{\text{train}}) + \sigma} \right).$$

Without loss of generality, let's compare $\lambda_1(\mathcal{K})$ and $\lambda_2(\mathcal{K})$. First we have that

$$\frac{1}{A_\kappa \lambda_1(C_{\text{train}}) + \sigma} < \frac{1}{A_\kappa \lambda_2(C_{\text{train}}) + \sigma}$$

as $A_\kappa > 0$ (follows from the Lemma above).

Furthermore, have

$$A_\kappa - \sigma B_\kappa = \frac{1}{\kappa}((\kappa - 1) - \sigma^2 \mathcal{M}'_\kappa(\sigma)).$$

We reason about this quantity as follows. We have that $A_\kappa - \sigma B_\kappa > 0$ as a result of this lemma, and so $(A_\kappa - \sigma B_\kappa)\lambda_2 \leq (A_\kappa - \sigma B_\kappa)\lambda_1$. Rearranging gives

$$\frac{B_\kappa \lambda_1(C_{\text{train}}) + 1}{A_\kappa \lambda_1(C_{\text{train}}) + \sigma} \leq \frac{B_\kappa \lambda_2(C_{\text{train}}) + 1}{A_\kappa \lambda_2(C_{\text{train}}) + \sigma}$$

and so we are done as we've shown $\lambda_1(\mathcal{K}) < \lambda_2(\mathcal{K})$ for $\lambda_1(C_{\text{train}}) > \lambda_2(C_{\text{train}})$.

For $\tau < 1$, $\tilde{\lambda} \neq 0$ and so the negative-definite contribution of $q\tilde{\lambda} F'_\kappa(\sigma)$ complicates the above argument. We provide preliminary numerical evidence for this case as follows. We compute $\tilde{\lambda}$ numerically from its self-consistency equation (21) to compute $\mathcal{K}$, of which we plot its eigenvalues against the eigenvalues of C_{train}. As demonstrated schematically in Figure 5, for τ values less than 1, it is consistently the case that the eigenvalues of $\mathcal{K}$ are negatively correlated with the eigenvalues of C_{train}. We emphasise that this is a heuristic check, and we plan to prove this rigorously in future iterations of this work.

E Trace Inequalities for Misalignment

In this appendix, we give a self-contained expository proof of Ruhe's trace inequality in the form we require for Corollary 4.1. We actually present two lines of analysis: first a direct proof of the inequality, and then an alternative analysis based on Riemannian optimization.

We begin by recalling the general setup: let A and B be $d \times d$ real symmetric matrices. By the spectral theorem, they are orthogonally diagonalizable, with non-increasingly ordered real eigenvalues $\lambda_1(A) \geq \lambda_2(A) \geq \cdots \geq \lambda_d(A)$ and $\lambda_1(B) \geq \lambda_2(B) \geq \cdots \geq \lambda_d(B)$, respectively. We want to show that

$$\sum_{j=1}^{d} \lambda_j(A)\lambda_{d-j+1}(A) \leq \operatorname{tr}(AB) \leq \sum_{j=1}^{d} \lambda_j(A)\lambda_j(B), \tag{E.1}$$

with equality attained in either bound if and only if A and B are co-diagonalizable.

Writing the eigendecompositions of A and B as

$$A = O_A \Lambda_A O_A^\top \quad \text{and} \quad B = O_B \Lambda_B O_B^\top, \tag{E.2}$$

respectively, where $O_A O_A^\top = I_d$, $O_B O_B^\top = I_d$, $[\Lambda_A]_{ij} = \lambda_i(A)\delta_{ij}$, and $[\Lambda_B]_{ij} = \lambda_i(B)\delta_{ij}$, we see immediately that it suffices to consider the case in which A is diagonal, with non-decreasing

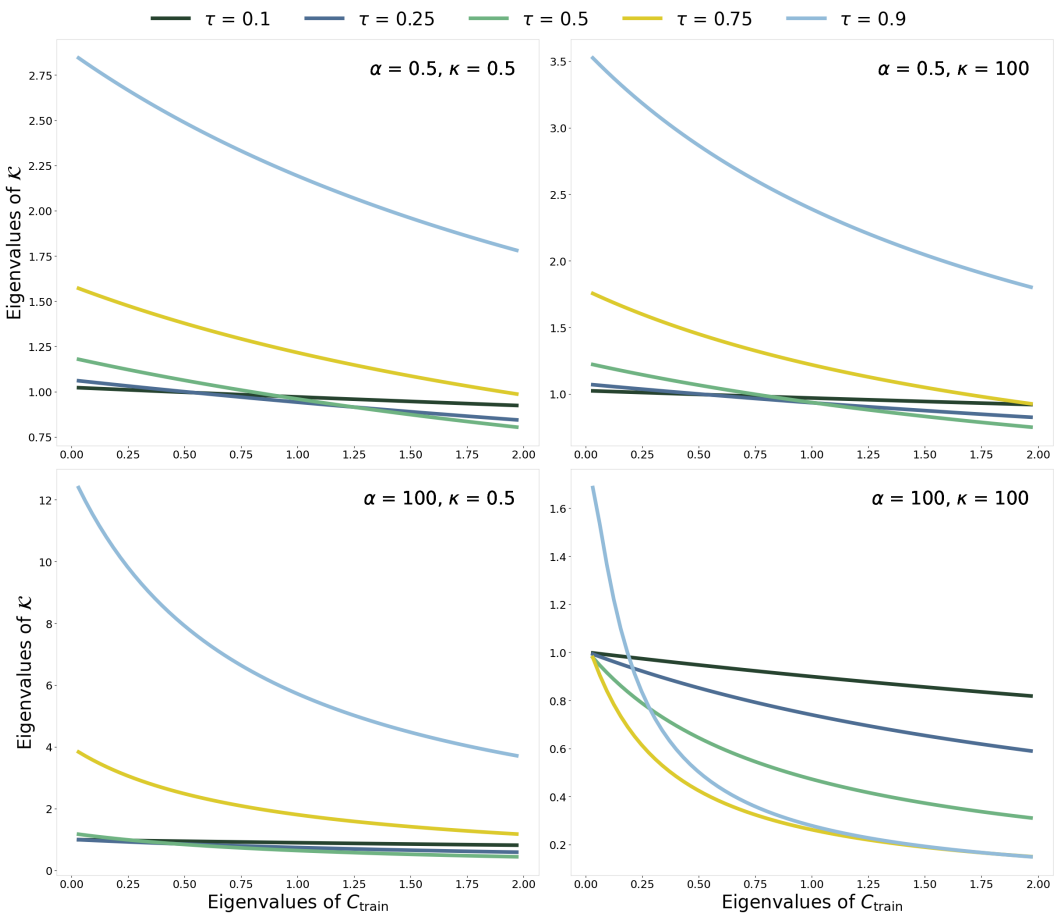

Figure 5: Demonstration of opposing eigenvalues for $\tau < 1$ values, at a range of κ and α values. C_{train} here is the same as in Figure 2, i.e. powerlaw spectrum.

elements, as

$$\text{tr}(AB) = \text{tr}(\Lambda_A O \Lambda_B O^\top) \quad \text{where} \quad O \equiv O_A^\top O_B, \tag{E.3}$$

and the matrix $O\Lambda_B O^\top$ has the same eigenvalues as B. We can see that A and B are co-diagonalizable if and only if $O\Lambda_B O^\top$ is diagonal. Moreover, we can see that the claimed bounds can be attained only if $O\Lambda_B O^\top$ is in fact equal to Λ_B up to pertmuation of its diagonal elements. What remains is to show that they are in fact bounds.

E.1 Direct proof of Ruhe's inequality

We now give a direct proof of the claimed inequality. We remark that the version of Ruhe's inequality proved in Marshall et al. (2010) is not sufficient for our purposes, as it assumes that both A and B are positive semi-definite, *i.e.*, that $\lambda_d(A) \geq 0$ and $\lambda_d(B) \geq 0$. We instead follow the proof for general Hermitian matrices outlined in Li (2020)'s blog post.

The strategy of this proof is to proceed by induction on the matrix dimension d. The claim clearly holds for $d = 1$, as then A and B are scalars equal to their only eigenvalue, and both bounds collapse. Now consider $d > 1$. Assuming—as noted before—that A is diagonal with elements given by its

ordered eigenvalues, we have

$$\operatorname{tr}(AB) = \sum_{j=1}^{d} \lambda_j(A) B_{jj} \tag{E.4}$$

$$= \sum_{j=1}^{d} [\lambda_j(A) - \lambda_d(A) + \lambda_d(A)] B_{jj} \tag{E.5}$$

$$= \sum_{j=1}^{d-1} [\lambda_j(A) - \lambda_d(A)] B_{jj} + \sum_{j=1}^{d} \lambda_d(A) B_{jj}. \tag{E.6}$$

We now observe that

$$\sum_{j=1}^{d-1} [\lambda_j(A) - \lambda_d(A)] B_{jj} = \operatorname{tr}(\Delta \tilde{B}), \tag{E.7}$$

where Δ is a $(d-1) \times (d-1)$ diagonal matrix with $\Delta_{jj} = \lambda_j(A) - \lambda_d(A)$ and $\tilde{B}$ is the $(d-1) \times (d-1)$ principal submatrix of B given by discarding its last row and column. The ordering of the eigenvalues of A implies the ordering

$$\lambda_1(A) - \lambda_d(A) \geq \cdots \geq \lambda_{d-1}(A) - \lambda_d(A) \geq 0 \tag{E.8}$$

of the eigenvalues of Δ.

Thus, $\operatorname{tr}(\Delta \tilde{B})$ is the trace of a product of $(d-1) \times (d-1)$ real symmetric matrices with Δ having its eigenvalues in non-decreasing order along the diagonal, so on the induction hypothesis we have the bound

$$\sum_{j=1}^{d-1} [\lambda_j(A) - \lambda_d(A)] \lambda_{d-j}(\tilde{B}) \leq \operatorname{tr}(\Delta \tilde{B}) \leq \sum_{j=1}^{d-1} [\lambda_j(A) - \lambda_d(A)] \lambda_j(\tilde{B}). \tag{E.9}$$

By the Poincaré separation theorem (also known as the Cauchy interlacing theorem), as $\tilde{B}$ is a principal submatrix of the real symmetric matrix B, we have the inequality

$$\lambda_{j+1}(B) \leq \lambda_j(\tilde{B}) \leq \lambda_j(B) \tag{E.10}$$

for all $j \in [d-1]$.

Combining these results and using the fact that $\lambda_j(A) - \lambda_d(A) \geq 0$ by our ordering assumption, we thus have the upper bound

$$\operatorname{tr}(AB) \leq \sum_{j=1}^{d-1} [\lambda_j(A) - \lambda_d(A)] \lambda_j(\tilde{B}) + \sum_{j=1}^{d} \lambda_d(A) B_{jj} \tag{E.11}$$

$$\leq \sum_{j=1}^{d-1} [\lambda_j(A) - \lambda_d(A)] \lambda_j(B) + \sum_{j=1}^{d} \lambda_d(A) B_{jj} \tag{E.12}$$

$$= \sum_{j=1}^{d-1} \lambda_j(A) \lambda_j(B) - \lambda_d(A) \sum_{j=1}^{d-1} \lambda_j(B) + \lambda_d(A) \sum_{j=1}^{d} B_{jj} \tag{E.13}$$

$$= \sum_{j=1}^{d-1} \lambda_j(A) \lambda_j(B) - \lambda_d(A) \sum_{j=1}^{d-1} \lambda_j(B) + \lambda_d(A) \sum_{j=1}^{d} \lambda_j(B) \tag{E.14}$$

$$= \sum_{j=1}^{d} \lambda_j(A) \lambda_j(B), \tag{E.15}$$

as $\operatorname{tr}(B) = \sum_{j=1}^{d} B_{jj} = \sum_{j=1}^{d} \lambda_j(B)$. Here, the first line uses the induction hypothesis in the form re-stated above, the second line uses the upper bound from the Poincaré separation theorem, and the remaining three lines are just algebraic simplification.

Similarly, we have the lower bound

$$\operatorname{tr}(AB) \geq \sum_{j=1}^{d-1}[\lambda_j(A) - \lambda_d(A)]\lambda_{d-j}(\tilde{B}) + \sum_{j=1}^{d}\lambda_d(A)B_{jj} \tag{E.16}$$

$$\geq \sum_{j=1}^{d-1}[\lambda_j(A) - \lambda_d(A)]\lambda_{d-j+1}(B) + \sum_{j=1}^{d}\lambda_d(A)B_{jj} \tag{E.17}$$

$$= \sum_{j=1}^{d-1}\lambda_j(A)\lambda_{d-j+1}(B) - \lambda_d(A)\sum_{j=1}^{d-1}\lambda_{d-j+1}(B) + \lambda_d(A)\sum_{j=1}^{d}\lambda_j(B) \tag{E.18}$$

$$= \sum_{j=1}^{d-1}\lambda_j(A)\lambda_{d-j+1}(B) - \lambda_d(A)\sum_{j=2}^{d}\lambda_j(B) + \lambda_d(A)\sum_{j=1}^{d}\lambda_j(B) \tag{E.19}$$

$$= \sum_{j=1}^{d}\lambda_j(A)\lambda_{d-j+1}(B). \tag{E.20}$$

By induction, we therefore conclude that

$$\sum_{j=1}^{d}\lambda_j(A)\lambda_{d-j+1}(B) \leq \operatorname{tr}(AB) \leq \sum_{j=1}^{d}\lambda_j(A)\lambda_j(B), \tag{E.21}$$

as desired.

E.2 Riemannian optimization

We now give an alternative perspective on this result based on the properties of orthogonal matrices. Consider

$$f(O) = \operatorname{tr}(\Lambda_A O \tilde{\Lambda}_B O^\top) \tag{E.22}$$

as a function on the space of orthogonal matrices, where $\tilde{\Lambda}_B$ is a diagonal matrix with non-zero elements given by any permutation of the eigenvalues of B. Near the identity, we can write any orthogonal matrix as

$$O = I + tS + \frac{1}{2}t^2S^2 + \mathcal{O}(t^3), \tag{E.23}$$

where S is a skew-symmetric matrix ($S^\top = -S$) and t is a small parameter. Substituting this expansion into $f(O)$, we have

$$f(O) = \operatorname{tr}(\Lambda_A\tilde{\Lambda}_B) - t\operatorname{tr}([\Lambda_A, \tilde{\Lambda}_B]S) + \frac{1}{2}t^2\operatorname{tr}(\Lambda_A\tilde{\Lambda}_BS^2 - 2\Lambda_AS\tilde{\Lambda}_BS + \Lambda_AS^2\tilde{\Lambda}_B) + \mathcal{O}(t^3), \tag{E.24}$$

where $[X, Y] = XY - YX$ is the matrix commutator. Irrespective of the permutation we have chosen to define $\tilde{\Lambda}_B$, $[\Lambda_A, \tilde{\Lambda}_B] = 0$, so $f(O)$ is stationary at the identity.

We therefore consider the quadratic term

$$H = \frac{1}{2}\operatorname{tr}(\Lambda_A\tilde{\Lambda}_BS^2 - 2\Lambda_AS\tilde{\Lambda}_BS + \Lambda_AS^2\tilde{\Lambda}_B), \tag{E.25}$$

as it will determine whether this stationary point is a local minimum, local maximum, or saddle. As $[\Lambda_A, \tilde{\Lambda}_B] = 0$, we can immediately simplify this to

$$H = \operatorname{tr}(\Lambda_A\tilde{\Lambda}_BS^2 - \Lambda_AS\tilde{\Lambda}_BS). \tag{E.26}$$

For brevity, define $a_i = (\Lambda_A)_{ii}$ and $b_i = (\tilde{\Lambda}_B)_{ii}$. Then, expanding in components,

$$H = \sum_{i,j=1}^{d}(a_ib_i - a_ib_j)S_{ij}S_{ji} \tag{E.27}$$

$$= -\sum_{i,j=1}^{d}a_i(b_i - b_j)S_{ij}^2, \tag{E.28}$$

as by skew-symmetry $S_{ji} = -S_{ij}$. Using the fact that the $i = j$ terms clearly vanish, we have

$$H = -\sum_{i<j} a_i(b_i - b_j)S_{ij}^2 - \sum_{i>j} a_i(b_i - b_j)S_{ij}^2. \tag{E.29}$$

By re-labling indices $i \leftrightarrow j$ and using the fact that $S_{ji}^2 = S_{ij}^2$,

$$\sum_{i>j} a_i(b_i - b_j)S_{ij}^2 = -\sum_{i<j} a_j(b_i - b_j)S_{ij}^2 \tag{E.30}$$

so upon re-combining terms

$$H = -\sum_{i<j}(a_i - a_j)(b_i - b_j)S_{ij}^2. \tag{E.31}$$

This now depends on the ordering of the eigenvalues, and thus on the permutation of indices. If the eigenvalues of both A and B are in non-increasing order such that $a_i \geq a_j$ and $b_i \geq b_j$ whenever $i < j$, we have $H < 0$, and the identity is a local maximum of $f(O)$. In contrast, if they are oppositely ordered, then $H > 0$ and the identity is a local minimum. Otherwise, the stationary point is a saddle. These results are consistent with Ruhe's inequality as proved above.

F Phase transition with increasing pretraining task diversity

As we have seen throughout, the task diversity parameter is crucial because it quantifies the quality of the pretraining data: higher κ implies a richer span of task variations, enabling the in-context learner to infer the structure shared between pretrain and test sets more accurately. Understanding κ thus sheds light on the implicit algorithm performed by the model. Previous work from Lu et al. (2025); Raventós et al. (2023) in particular have investigated the performance of ICL as κ increases. In particular, Lu et al. (2025) showed, in the isotropic task case, that there is a phase transition at $\kappa = 1$: for $\kappa < 1$, the model has insufficient task diversity to be able to generalize within tasks, and is forced to memorize the training tasks, while for $\kappa > 1$, the model has seen sufficient tasks to generalize in-context efficiently.

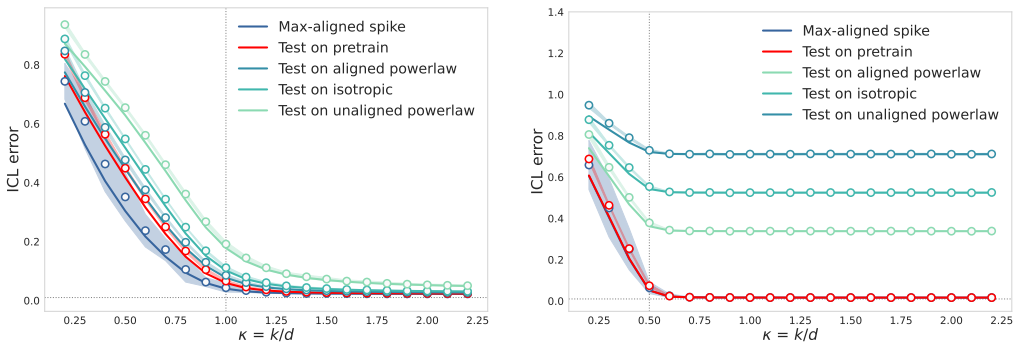

(a) Full-rank phase transition (b) Half-rank phase transition

Figure 6: Theory curves with corresponding numerical simulations showing phase transition of ICL error in κ for a range of test structures. For (a) C_{train} is the same as in Figure 1 and is full-rank; for (b) $C_{\text{train}} = \text{diag}[2I_{d/2}, 0_{d/2}]$, thus half-rank. *Parameters:* $d = 80, \alpha = 80, \tau = 80, \rho = 0.01$. Tests for each are done on C_{train}, I_d, powerlaw (spectral power 0.5, aligned and unaligned with C_{train}), as well as the rank-1 C_{test} optimal from Result 4.2.

The settings considered in both Lu et al. (2025); Raventós et al. (2023) focus on isotropic tasks where the pretraining and testing task distributions are the same. Here, we verify that not only does this phase transition in task-diversity remain in the presence of structured pretraining task distributions, but further is independent of the test distribution (see Figure 6).

Corollary F.1: Phase transition in task diversity

In the proportional limit of $\alpha, \tau \to \infty$ such that $\tau = \alpha/\gamma$ for $\gamma = \Theta(1)$ fixed, there is a phase transition in e_{ICL} at $\kappa = \text{rank}(C_{\text{train}})/d$. Specifically, for $r \equiv \text{rank}(C_{\text{train}})/d$ then

$$\lim_{\tau,\alpha\to\infty} e_{\text{ICL}}(C_{\text{train}}, C_{\text{test}}) = \begin{cases} \rho + \left(1 + \frac{\rho}{\rho + c_{\text{train}}}\gamma\right) \text{tr}\left[C_{\text{test}} \left(x_1 C_{\text{train}} + I_d\right)^{-1}\right] & \kappa < r \\ \rho + \left(1 + \frac{\rho}{\rho + c_{\text{train}}}\gamma\right) \text{tr}\left[C_{\text{test}} \left(x_2 C_{\text{train}} + I_d\right)^{-1}\right] & \kappa > r \end{cases} \tag{F.1}$$

where x_1 and x_2 are defined self-consistently as solutions of

$$\text{tr}\left[\left(x_1 C_{\text{train}} + I_d\right)^{-1}\right] = 1 - \kappa \tag{F.2}$$

$$\text{tr}\left[\left(x_2 C_{\text{train}} + I_d\right)^{-1}\right] = 1 - r. \tag{F.3}$$

To prove this result, we first suppose that C_{train} is invertible. We start by writing the self-consistency equation

$$\mathcal{M}_\kappa(\sigma) = \frac{1}{d} \text{tr}\left(\left(\left(1 - \frac{1}{\kappa} + \frac{\sigma}{\kappa}\mathcal{M}_\kappa(\sigma)\right) C_{\text{train}} + \sigma I_d\right)^{-1}\right). \tag{F.4}$$

for $\mathcal{M}_\kappa(\sigma)$ equivalently as a self-consistency equation for the renormalized ridge $\tilde{\sigma}$, defined by

$$\tilde{\sigma}\, \text{tr}[(C_{\text{train}} + \tilde{\sigma})^{-1}] = \sigma \mathcal{M}_\kappa(\sigma)$$

or equivalently

$$\tilde{\sigma} = \frac{\sigma}{1 - \frac{1}{\kappa} + \frac{\tilde{\sigma}}{\kappa} \text{tr}\left[(C_{\text{train}} + \tilde{\sigma})^{-1}\right]}. \tag{F.5}$$

In the $\sigma \to 0$ limit, $\tilde{\sigma}$ limits to 0 when $\kappa > 1$, and limits to the unique solution of

$$1 - \frac{1}{\kappa} + \frac{\tilde{\sigma}}{\kappa} \text{tr}\left[(C_{\text{train}} + \tilde{\sigma})^{-1}\right] = 0 \tag{F.6}$$

for $\kappa < 1$. For our purposes, this means that

$$\lim_{\sigma\to 0} \sigma \mathcal{M}_\kappa(\sigma) = \begin{cases} 1 - \kappa\,, & \kappa < 1 \\ 0\,, & \kappa > 1 \end{cases} \tag{F.7}$$

as well as

$$\lim_{\sigma\to 0} \sigma F_\kappa(\sigma) = \lim_{\sigma\to 0} \left(\frac{1}{\sigma}\left(1 - \frac{1}{\kappa} + \frac{\sigma \mathcal{M}_\kappa(\sigma)}{\kappa}\right) C_{\text{train}} + I_d\right)^{-1} \tag{F.8}$$

$$= \begin{cases} \left(x C_{\text{train}} + I_d\right)^{-1}, & \kappa < 1 \\ 0\,, & \kappa > 1 \end{cases} \tag{F.9}$$

and finally

$$\lim_{\sigma\to 0} \sigma^2 F'_\kappa(\sigma) = \begin{cases} -\left(x C_{\text{train}} + I_d\right)^{-1}, & \kappa < 1 \\ 0\,, & \kappa > 1 \end{cases} \tag{F.10}$$

for x defined by $\text{tr}\left[\left(x_1 C_{\text{train}} + I_d\right)^{-1}\right] = 1 - \kappa$.

Using these characterizations of the $\sigma \to 0$ limit, and noticing for our problem that if $\tau \to \infty$ (so $\tilde{\lambda} = 0$), then we must take the $\sigma \to 0$ limit of e_{ICL}, being careful to use

$$\tau = \frac{\rho + c_{\text{train}}}{\gamma} \frac{1}{\sigma} \tag{F.11}$$

to enforce the proportional α/τ limit. Doing so gives the required answer.

The above proof requires explicitly that C_{train} is invertible. If it is not, we have to be more careful with handling the $\sigma \to 0$ limit of (D.4). One potential branch of this solution is

$$1 - \frac{1}{\kappa} + \frac{1}{\kappa}\tilde{\sigma}\, \text{tr}[(C_{\text{train}} + \tilde{\sigma})^{-1}] \to 0 \tag{F.12}$$

or equivalently

$$\frac{1}{d}\sum_{i=1}^{r}\frac{\tilde{\sigma}}{\lambda_i+\tilde{\sigma}}+\frac{1}{d}(d-r)\frac{\tilde{\sigma}}{0+\tilde{\sigma}}\to 1-\kappa \quad\Longrightarrow\quad \frac{1}{d}\sum_{i=1}^{r}\frac{\tilde{\sigma}}{\lambda_i+\tilde{\sigma}}\to\frac{r}{d}-\kappa \tag{F.13}$$

where r is the rank of C_{train}. This is what causes the split in behavior of the solution at $\kappa = r/d$ (which was previously 1). For $\kappa < r/d$, this is solvable at nonzero $\tilde{\sigma}$ and we end up with the familiar solution branch of

$$\sigma\mathcal{M}_\kappa(\sigma)=\tilde{\sigma}\,\mathrm{tr}[(C_{\text{train}}+\tilde{\sigma})^{-1}]\to 1-\kappa. \tag{F.14}$$

For $\kappa > r/d$, there is no longer a sensible solution at nonzero $\tilde{\sigma}$ (since $\tilde{\sigma}$ cannot be negative) and so we're forced to take $\tilde{\sigma}\to 0$. This gives

$$\sigma\mathcal{M}_\kappa(\sigma)=\tilde{\sigma}\,\mathrm{tr}[(C_{\text{train}}+\tilde{\sigma})^{-1}]=\frac{1}{d}\sum_{i=1}^{r}\frac{\tilde{\sigma}}{\lambda_i+\tilde{\sigma}}+\frac{1}{d}(d-r)\frac{\tilde{\sigma}}{0+\tilde{\sigma}}\to 1-\frac{r}{d}\,. \tag{F.15}$$

This concludes the proof of the claimed result, and recovers the previous result for invertible C_{train}.

G Context length shifts

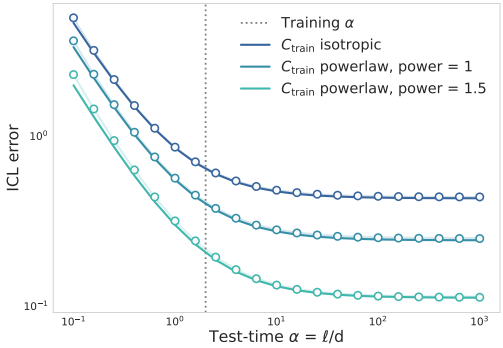

Figure 7: Theory curves with corresponding numerical simulations showing monotonicity of error in test-time context length for a variety of task structures. The dashed line corresponds to training α. *Parameters*: $d = 150$, $\alpha = 2$, $\tau = 4$, $\kappa = 1$, $\rho = 0.01$. Testing is done on the same distribution as pretraining.

We have thus far assumed that the pretraining- and test-time context lengths are the same. Our general result in (C.2) allows for an α_{test} that differs from the training context length α, but shows that this shift only affects a single scaling factor in e_{scalar}, where a factor of $1/\alpha$ is replaced by $1/\alpha_{\text{test}}$. Despite e_{ICL} not being monotonic in training context length, as demonstrated by Lu et al. (2025), it is monotonically decreasing in test context length: testing on larger-context prompts can only decrease error, and testing on shorter-context prompts can only increase error. This is demonstrated in Figure 7 for a variety of different task structures. Recall that α_{test} only appears in e_{ICL} through e_{scalar}, as part of an effective noise term: having longer test-time contexts will give the model a better estimate of the token distribution, leading to a better predictor for the task corresponding to that context.

H Experimental details

All code will be provided upon acceptance.

H.1 Linear Simulations

Linear simulations are done by sampling pretraining and testing distributions as described by (2) and (12), and computing numerical Γ^* by (B.1). We simulate the ridgeless $\lambda \to 0$ limit of this theory by taking $\lambda = 0.00001$.

H.2 NONLINEAR ARCHITECTURE

The architecture used for Figure 3 is a transformer formed of two transformer-blocks, constructed as follows. The input to the architecture is the Z matrix (3). We apply a causal mask to ensure that each token attends to itself and prior tokens in the sequence. Each transformer-block is made of first applying single-head softmax attention to this masked input, with residual connection, and then normalised; this is then passed to a single hidden layer MLP with GELU activation, followed by a final residual connection and layer norm application. The final logit is computed by a dense layer projecting the output of the two transformer-blocks into a scalar.

The model is pretrained with data sampled by (2). We form n Z-matrices from these samples, which are again the inputs to the architecture, and the model is pretrained to predict the corresponding $y_{\ell+1}$ value by minimising MSE loss between the final logit and $y_{\ell+1}$. Training is done using AdamW for 1000 epochs with batch size 16 and learning rate 0.0001.

Testing is done by sampling a batch of n contexts from (12), and tracking MSE between the true $y_{\ell+1}$ and the model output. This test sampling is repeated 500 times to average out noise.